1 Report No	2. Government Accession No	3 Recipient's Catalog No.
NASA CR- 177362		

4 Title and Subtitle	5. Report Date
Estimation of Dynamic Rotor Loads for the Rotor Systems Research Aircraft: Methodology Development and Validation	May, 1985
	6. Performing Organization Code: FHF
7 Author(s): R. W. Du Val and M. Bahrami	8 Performing Organization Report No
	10 Work Unit No.: Job Order # T4713D
9 Performing Organization Name and Address: Advanced Rotorcraft Technology, Inc. 1804 Stierlin Road, Suite 210 Mountain View, CA 94043	11 Contract or Grant No: NAS2-11688
	13 Type of Report and Period Covered: Contractor Report
12 Sponsoring Agency Name and Address: National Aeronautics and Space Administration Ames Research Center, Moffett Field, CA 94035	14 Sponsoring Agency Code: RTOP # 505 4251

15 Supplementary Notes

Point of Contact: Technical Monitor, C. W. Acree, M.S. 237-3, NASA Ames Research Center, Moffett Field, CA 94035 (415) 694-5664 or FTS 464-5664

16 Abstract

The Rotor Systems Research Aircraft uses load cells to isolate the rotor/transmission system from the fuselage. A mathematical model relating applied rotor loads and inertial loads of the rotor/transmission system to the load cell response is required to allow the load cells to be used to estimate rotor loads from flight data. In this study, such a model is derived analytically by applying a force-and-moment balance to the isolated rotor/transmission system. The model is tested by comparing its estimated values of applied rotor loads with measured values obtained from a ground based shake test. Discrepancies in the comparison are used to isolate sources of unmodeled external loads.

Once the structure of the mathematical model has been validated by comparison with experimental data, the parameters must be identified. Since the parameters may vary with flight condition it is desirable to identify the parameters directly from the flight data. A Maximum Likelihood identification algorithm is derived for this purpose and tested using a computer simulation of load cell data. The identification is found to converge within 10 samples. The rapid convergence facilitates tracking of time varying parameters of the load cell model in flight.

17 Key Words (Suggested by Author(s))	18 Distribution Statement
Aeronautics, Load Cell, Dynamic, Calibration, Rotor Systems Research Aircraft, Parameter Identification	Unclassified - Unlimited Subject Category 05

19 Security Classif (of this report)	20 Security Classif (of this page)	21 No of Pages	22. Price*
Unclassified	Unclassified	50	

*For sale by the National Technical Information Service Springfield Virginia 22161

NASA CONTRACTOR REPORT 177362

(NASA-CR-177362) ESTIMATION OF DYNAMIC ROTOR LOADS FOR THE ROTOR SYSTEMS RESEARCH AIRCRAFT: METHODOLOGY DEVELOPMENT AND VALIDATION (Advanced Rotorcraft Technology, Inc.) 56 p HC A04/MF A01 CSCL 01C G3/05

N85-31045

Unclas 24912

Estimation of Dynamic Rotor Loads for the Rotor Systems Research Aircraft: Methodology Development and Validation

R. M. Du Val
M. Bahrani

CONTRACT NAS2- 11688
MAY 1985

NASA

NASA CONTRACTOR REPORT 177362

Estimation of Dynamic Rotor Loads for the Rotor Systems Research Aircraft: Methodology Development and Validation

R. W. Du Val and M. Bahrami
Advanced Rotorcraft Technology, Inc.
Mountain View, California
May, 1985

Prepared for
Ames Research Center
under Contract NAS2-11688

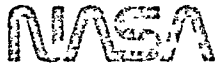

National Aeronautics and
Space Administration

Ames Research Center
Moffett Field, California 94035

TABLE OF CONTENTS

LIST OF TABLES AND FIGURES

INTRODUCTION

The Rotor Systems Research Aircraft (RSRA) has a set of seven load cells connecting the main rotor transmission to the fuselage Their purpose is to make high accuracy measurements of the net rotor loads as resolved at the rotor hub from flight data 1. The use of these load cells to estimate applied rotor forces and moments at the hub requires an accurate mathematical expression relating rotor loads, inertial loads and load cell readings Both the structure and parameters of this model must be specified Previous approaches to processing ground test data have not yielded an acceptably accurate relationship for the case of high frequency dynamic loads

The previous approaches have utilized empirical techniques based on experimental data to obtain the desired model The approach presented in the first phase of this study is to develop the model analytically and validate it from experimental data using modern techniques of model structure determination and parameter identification This approach provides a level of physical insight that has been missing in the purely experimental approaches and the resulting analytical relationship provides a unified basis for utilizing both static and dynamic calibration data to validate and upgrade a common model

The second phase of this study develops and demonstrates a technique for identifying the parameter values of the model directly from flight data thereby eliminating a costly ground test procedure and potentially providing more accurate results than could be obtained from ground based calibration The capability to provide "active sensor calibration" in an operational environment has potential applications beyond the RSRA load cell problem

NOMENCLATURE

Symbols

u . .. Input

y .. Output

N_b ... . Number of rotor blades

Ω . . . Rotor rate (rad sec)

$\vec{H}$. Vector of 6 applied hub loads

$\hat{H}$ .Estimates of applied hub loads

$\vec{T}$. ... Vector of 7 load cell measurements

$\vec{J}$. Vector of 6 inertial loads

$\vec{\Theta}$. Set of unknown parameters

$\hat{\Theta}$. . A-priori estimate of parameters

$\dot{\Theta}$ Post-calibration estimate of parameters

$\vec{\alpha}$ Set of 11 load cell deformation angles

$\hat{\alpha}$ Pre-identification estimate of $\vec{\alpha}$

$\dot{\alpha}$ . . . Post-identification estimate of $\vec{\alpha}$

it Longitudinal rotor shaft tilt

S . Transformation matrix for load cells

R . .. Transformation matrix for hub loads

$E\{\}$ Expected value operator

$\vec{\nu}$ Vector of measurement noise components

Q_ν . Co-variance of measurement noise components

$\vec{\eta}$ .. Vector of process noise components

Q_η. . Co-variance of process noise components

$\vec{x}$. Vector of states to be estimated

$\hat{x}$ . . Estimate of state vector

F . Dynamic coupling matrix for states

Φ . . Transition matrix for states

n .... Index of measurement update times

Δt Time between measurement updates

J_x . . Partial derivative of inertial loads w r t states

J_a Partial derivative of inertial loads w r t deformation angles

P. . Co-variance of state estimation error

K Kalman gains

V. Maximum Likelihood cost function

W . . Measurement error weighting matrix .

N_s Number of samples used for identification

$\bar{e}_J$. . Error in estimate of inertial loads

$\bar{e}_H$ Error in estimate of applied hub loads

ω . Frequency

A, B, C, D, E, F, G Individual load cell outputs (Fig A 1)

X, Y, Z, L, M, N . Force and moment components (Fig A 2)

b Position of C G from shaft attach point

h . Position of hub from C G

l . Position of C G from aft load cell attach points

c . Lateral offset of forward lateral load cell from centerline

f . . Lateral offset of aft lateral load cell from centerline

w Lateral distance between vertical load cell attach points

d. Longitudinal distance between vertical load cell attach points

$\phi.\theta.\psi$ Load cell deformation angles about x, y and z axes respectively

$\bar{a}$ . . . Linear acceleration at C G

I . Moment of inertia about C G

m . . . . Effective mass of rotor/transmission engine system

M . Mass matrix

p, q, r . . . Rotational rates about x, y, and z axes

Q_t . Total applied engine and tail rotor drive torques

$\Gamma_{\ldots}$. Gyroscopic coupling coefficients

Subscripts

A . Accelerometer

i, j Row and column indices respectively for vectors and matrices

o Low frequency component

1 One rev component

N . N_b rev component

m Measured data

x, y, z Component for x y, z axis

I Inertial load

H Hub load

C Total load

T Load Cell

a, b c, d, e, f, g Attach point of each load cell

Superscripts

$-$ Pre-measurement estimate

$-$ Post-measurement estimate

PHASE I: DEVELOPMENT AND VALIDATION OF AN ANALYTICAL MODEL OF THE ROTOR/TRANSMISSION/LOAD-CELL SYSTEM

Background

Previous Methods

The initial attempt to determine the load cell response to the applied rotor loads involved applying static loads at the hub and measuring the resulting load cell response. A least squares regression approach was used to identify a coefficient matrix relating the seven load cells to the six hub loads. A six element bias vector was also estimated. It was found [2] that the coefficient matrix varied as a function of the applied multiple axis load. This indicates either a nonlinear dependence of the load cell response to the applied rotor loads or an unmodeled independent variable in the regression.

The next calibration was a ground based shake test in which a pair of inertial shakers were mounted on the rotor hub to apply dynamic loads at specified amplitudes and frequencies [3]. During this experiment, the RSRA was suspended from the hub, so the static loading was the same for all tests. As a result, the nonlinear variation of the relationship with static loads, as observed in the static test, should not have been present in the shake test. The Force Determination Method [4] was utilized to estimate applied rotor loads from a variety of sensors around the aircraft. This method first identifies the transfer functions between the applied rotor loads and sensors at various points on the aircraft and then identifies the applied rotor load from a least squares fit to the transfer functions and measured sensor responses. The results were unacceptable because the identified transfer functions varied with the magnitude of the applied load, hence they could not be used to estimate the applied load without some extensive calibration procedure. Again, the variation with applied rotor load indicates either a nonlinear dependence or an unmodeled load source.

Proposed Method

Since the sensors utilized in the Force Determination Method included numerous accelerometers and strain guages mounted on the fuselage, transfer functions of these sensors will be affected by any nonlinear dynamic behavior in the fuselage. This effect complicates the use of sensors on the fuselage to determine applied rotor loads. The RSRA was designed to use load cells to isolate applied loads from different sources, such as the main rotor, tail rotor, engine and wings. The proposed approach takes advantage of this concept by treating the rotor transmission as an isolated system with externally applied loads from the load cells and the rotor (Fig. 1). The applied rotor loads are then measured from a force and moment balance using measured load cell loads ($\vec{T}$) and inertial loads ($\vec{J}$) as derived from transmission accleration measurements. In order to utilize this approach, a model is required that relates applied external loads on the rotor/transmission system to the resulting forces and moments at the center of mass of the system. This model is derived analytically from physical principles, using the known geometry of the rotor/transmission system. Potentially uncertain parameters in this model are explicitly represented to provide the capability to calibrate the model.

The advantages of this approach predominantly arise from the physical insight obtained in using an analytically derived model. With such a model, sensitivity analysis and physical judgement can be used to select the most appropriate set of available parameters for calibration. Consequently, fewer parameters need be calibrated than when no physical insight is used. In addition, the parameters to be calibrated now have a physical interpretation so the validity of the calibration results may be assessed. The model

should initially be derived to be as simple as possible If it can not adequately explain the observed experimental behavior with a physically reasonable set of parameter values, it may be expanded to include additional effects as required It is important that all major effects be identified and incorporated into the model before calibration of the parameters is attempted, or the parameter values will compensate for the unmodeled effects as best they can and achieve physically unrealistic values in the process

Objective and Approach

The objective of this phase of the study is to derive a simple dynamic model of the isolated rotor/transmission system and test its accuracy with experimental data The approach is to first derive a simple model of the rotor transmission system, treating it as a linear, rigid isolated body Known or assumed values are used for all parameters of the derived model The model is then applied to test data to determine its accuracy If it appears that calibration can further improve the accuracy, the appropriate parameter set will be selected and calibrated If the accuracy appears limited by an unmodeled effect, the model will be expanded to evaluate potential sources of the unmodeled effect

Rotor/Transmisssion Model

The arrangement of the load cells below the rotor transmission system is shown in Fig 2 A detailed description of this system, including all inertia contributions is given in Reference 2 There are seven load cells, four of them mounted vertically at the corners of the transmission mounting plate, two mounted laterally along the fore and aft edges of the mounting plate and one mounted longitudinally at the forward edge of the mounting plate An inertial load vector, $\vec{J}$, is located at the center of gravity of the rotor/transmission system and the applied rotor load vector (H) is located at the rotor hub (Fig. 3) The rotor hub is located at the end of the rotor shaft which is tilted forward at an angle of 2 degrees The load cells are connected to the transmission and the fuselage by spherical bearings

The proposed approach is to estimate the applied hub loads from a force and moment balance of the external loads and the inertial loads In order to accomplish this all externally applied loads must be transformed to the center of mass, where the inertial loads act By treating the rotor transmission as an isolated system, the load cell forces are considered a measured, externally applied load on the system A 6x7 matrix (S) is derived that transforms the vector of seven load cell loads ($\vec{T}$) at their attach points to a set of 6 load components at the center of mass A 6x6 matrix (R) is derived that transforms the vector of applied rotor loads ($\vec{H}$) at the hub to the center of mass An inertial load vector ($\vec{J}$) at the center of mass is derived from measured accelerations and assumed inertial parameters. Using the derived matrices,a force and moment balance at the center of mass results in a set of six simultaneous equations which may be written in matrix form as

$$\vec{J} - S\vec{T} - R\vec{H} = 0 \qquad (1\ 1)$$

A detailed description of these vectors and matrices are given in Appendix A

The assumptions used in deriving the matrices and Eq 1 1 are that the rotor/ transmission system is a rigid body and that there is no friction in the load cell bearings These assumptions were made to simplify the initial approach Both non-rigid body effects and friction in the load cell bearings could be added to the model if that appears to be required in order to match the experimental data

The transformation matrices S and R and the inertial load vector $\vec{J}$ were all derived to explicitly contain all potentially uncertain parameters of the system so that any subset of parameters can be selected for calibration, as required to improve the model accuracy The parameters explicitly defined in the model are

a) All distances and angles required to define the resultant moment arm from the center of mass to load application points

b) All angles and magnitudes required to define load cell load components acting on the rotor/ transmission system

c) All mass properties required to determine inertial loads from measured rates and accelerations

Test Conditions

Having derived a model, the next step is to evaluate it with experimental data Both static and dynamic ground test data are available The dynamic data generated by the shake test were chosen since it would provide a more rigorous test of the model structure than the static test data The dynamic data are not, however, suitable for testing the calibration procedure This is because the same static load condition exists for all dynamic tests and parameter variations are mostly dependent on variations in the static loading Once the model structure has been validated with the dynamic data the model can be applied to the static test data to evaluate the calibration procedure

The test data set selected was a frequency sweep from 15 to 18 5 Hz in the applied rotor load. This frequency range was chosen because it contains the N_b rev frequency, and identification of applied rotor loads at this frequency is of special interest Transfer function data were generated from the raw test data by a harmonic analyzer for four levels of applied load in each of the three axes Eq 1 1 was then used to generate the applied load estimate from the transfer function data Eq 1 1 was processed with the values of all of the model parameters set to their design specifications

Error Analysis

Total Estimation Error

In a controlled ground test environment, the actual values of the applied rotor loads are known so the total error in the estimate is readily obtained Given the vector of measured load cell readings $\vec{T}_m$, and the vector of inertial loads derived from accelerometer measurements $\vec{J}_m$, Eq 1 1 may be used to estimate the applied rotor loads as

$$\hat{\vec{H}} = -R^{-1}\,\vec{J}_m - S\vec{T}_m \tag{1 2}$$

The total error in the estimate is obtained by subtracting the known values of applied rotor load from the estimate of Eq 1 2 to get

$$\vec{e}_H = \hat{\vec{H}} - \vec{H} = -R^{-1}\,\vec{J}_m - S\vec{T}_m - \vec{H}$$

$$\vec{e}_H = -R^{-1}\,\vec{J}_m - S\vec{T}_m - R\vec{H} \tag{1 3}$$

The available shake test data was in the form of transfer functions that had been generated from the raw data by a harmonic analyzer. In order to utilize this data with the proposed model it was necessary to transform the model to the frequency domain and write it in terms of the transfer functions. Transforming Eq. 1.3 to the frequency domain gives.

$$\bar{\epsilon}_H(\omega) = -R^{-1}\bar{J}_m(\omega) - S\bar{T}_m(\omega) - R\bar{H}(\omega) \tag{1.4}$$

If only a y-axis rotor load, $H_y(\omega)$, is applied, Eq. 1.4 may be written in terms of the transfer functions as

$$\bar{\epsilon}_H(\omega) = -R^{-1}\left(\frac{\bar{J}_m(\omega)}{H_y(\omega)}\right) - S\left(\frac{\bar{T}_m(\omega)}{H_y(\omega)}\right) - R\,H_y(\omega) \tag{1.5}$$

where $\frac{\bar{J}_m(\omega)}{H_y(\omega)}$ and $\frac{\bar{T}_m(\omega)}{H_y(\omega)}$ are vectors of transfer functions of the inertial and load cell loads with respect to the y-axis rotor load. Eq. 1.5 was used to evaluate the total error in the estimate using the available transfer function data for y-axis excitation. Corresponding expressions were used to evaluate the estimation error for x and z axis excitations. The effect of applied moments at the rotor hub was not evaluated in this study.

Numerous potential sources of error are present in this system. The evaluation procedure was to examine the total error and attempt to categorize it into the potential sources. Once identified, the sources would be modeled and included in the system. Most of the error will probably be atttributable to one of five sources.

1) Systematic errors in data collection

2) Unmodeled static and dynamic effects

3) Unmodeled external loads

4) Random errors in sensors

5) Incorrect parameter values

Systematic Errors in Data Collection

One source of error is the use of transfer function data. Since this is treated as raw data in this study any errors in the identification of the transfer functions would propagate through the proposed approach. The recorded time domain data should be reprocessed by the harmonic analyzer to provide only Fourier transformed data, not transfer functions.

Angular accelerometers and rate gyros were not available on the rotor transmission system for the shake test. Since there is no way to obtain angular acceleration data, the approach taken is to assume its values are negligible and see how good the estimates are with this assumption. Some justification for this assumption comes from comparing the response of two linear accelerometers that are mounted on the transmission with a two foot vertical displacement between them. The difference in the y-axis components divided by the vertical displacement should give the roll axis angular acceleration. The average

value of this derived roll acceleration over the frequency range was found to be 09 rad sec sec, supporting the low angular acceleration assumption The derived angular acceleration data was not used with the model because the errors in the linear accelerometers are such that the accuracy of the derived angular acceleration is 6 rad, sec sec. The derived values are therefore in the noise level The anguar acceleration affects the translational equations since the linear accelerometer is not mounted at the center of mass and will therefore be affected by angular accelerations The moment equations are affected since the angular inertial loads are dependent on the angular acceleratons The errors associated with neglecting a 09 rad sec sec roll angular acceleration are 12 lbs in the y force and 27 ft lbs in the rolling moment so the assumption appears justified

Unmodeled Static And Dynamic Effects

The model derived for this study was kept deliberately simple to facilitate the analysis It can be expanded if necessary to account for the observed error Unmodeled effects with potentially significant impact on the model include friction in the load cell bearings flexibility in the rotor/transmission system and nonlinearity in the dynamic response to applied loads The nature of the error signal should suggest which of these effects are present Friction and deadbands will be characterized by hysteresis in the response This effect is more readily observed in static data than in dynamic data Flexibility will show up as a resonance at some frequency and will result in a phase and amplitude shift between the input and output signals Nonlinear dynamics will be readily detected by a frequency shift between the input and output data Static nonlinearities result in parameter variations and are corrected by calibration rather than by expanding the model

Random Errors In Sensors

Both load cells and accelerometers have measurement noise which produces a lower bound on the accuracy of the applied load estimates It is possible to obtain accuracies in excess of this limit but this requires the use of statistical processing techniques such as Kalman Filtering and Smoothing This effect can not be reduced by any modifications to the model The effect of accelerometer and load cell noise on the applied rotor load estimate is derived in Appendix B and used to generate the errors given in Table I This table compares the estimation errors in each axis for four levels of applied load with the predicted standard derivation of the error based on instrumentation noise These numbers were based on the assumption of independent random errors for each sensor with accuracies of 1 percent of full scale for the accelerometers and 0 1 percent of full scale for the load cells The total instrumentation error is shown along with the components ddue to load cell and accelerometer noise

Table I

	Estimation error				Instrumentation noise		
Load	200lb	400lb	600lb	800lb	Total	Load cells	Accel
X	84	76	173	211	309	25	308
Y	10	25	35	96	312	35	308
Z	1 2	17	28	39	312	30	308
L	592	1618	1772	2177	446	179	408
M	27	17	24	47	136	143	412
N	81	76	173	214	81	61	51

Load cell full scale = 25,000 lb , err = 1%
Accelerometer full scale 7 G's , err = 1%
Mass = 1400 lb

Unmodeled External Loads

The derived model will be in error if any externally applied load is not included If the levels are low, then this can be the most difficult source of error to identify This is because it can take on virtually any characteristics and will blend in with other error sources. The only possibility for detecting this type of error is if it is sufficiently large that it can not be logically explained by any of the other error sources. Once the presence of an unmodeled load is suspected, the error data may assist in isolating its source, but a thorough examination of the test condtions is usually required to resolve this effect

Incorrect Parameter Values

Once the model structure has been validated to the fullest extent possible, the remaining errors should be due only to incorrect values for the parameters At this point calibration may be applied to reduce this error source. If calibration is attempted before the model structure is adequately determined , the parameters will take on whatever values are required to compensate for the model structure errors This will result in physically unrealistic values for the parameters and could, in fact, be a test for whether the model structure is accurate

The conventional approach to calibration has been to apply least squares minimization of the error with respect to the parameters to be calibrated Since the parameters are now imbedded in a model, the least squares minimization of the error must be done subject to the constraint that the model equations are satisfied This is refered to as a constrained least squares approach [5], and the algorithm is derived in Appendix C for the constraint of Eq 1 1

Since the available data is in the frequency domain, the calibration must be performed in the frequency domain This is actually an advantage since the frequency domain transformation has concentrated information for the required frequency range into fewer data points than required for a time domain representation Calibration may then be performed with less data in the frequency domain. The least squares minimization may be applied to frequency domain data in the same way as it is applied to time domain data [6] The only modification is that the data is organized with the real and imaginary parts stacked end to end rather than using the data in complex form This insures that the identified parameter values will not be complex

Results

Eq 1 3 was applied to transfer function data for the load cells and the main rotor gear box accelerometers to generate the estimation error of the derived model in the frequency domain The values used in the design specification for the geometry and mass properties were used for all parameters in the model Fig's 4 and 5 show the magnitude of the transfer function data for the 7 load cells and 3 accelerometers for an 800 lb y-axis excitation The location of the load cells may be seen by finding the correspondingly labeled load cell in Fig 2 The accelerometer transfer functions have been multiplied by the system mass to produce inertial loads The strong coupling in the system is apparent from the large vertical load cell values for a y-axis excitation The strong correlation in the z-axis is particularly apparent from the sudden drop in z-axis acceleration at the same frequency (16 6 Hz) where two vertical load cells (A and B) suddenly assume equal and opposite values

Figures 6 through 11 show the six axis estimation errors for y-axis excitation at 200, 400, 600 and 800 pound levels to demonstrate the effect of load level on estimation error. The flight values of the applied the applied rotor load at the N_b/rev frequency should fall within this range Figures 12 through 17 show the

six axis estimation errors for x, y, and z axis excitation at the 400 pound level to demonstrate the effect of excitation axis on the estimation error. The errors plotted in (Figures 6 through 17) were obtained from Eq. 1.3 using nominal parameter values. Table I shows the average error over the frequency range as compared to the accuracy limit set by the instrumentation noise. With the exception of applied rolling moment due to y-axis excitation and x-axis force due to x-axis excitation, the average error shown in Table I and the frequency plots comparing the three axes of excitation shown in Fig's 12-17, demonstrate that the rigid body model of the isolated rotor transmission system produces applied load estimates with error levels comparable to the instrumentation noise level.

The pronounced roll moment error from y-axis excitation (Fig. 15) is too great to be explained by parameter errors, sensor errors or angular accelerations. The demonstrated lack of significant angular accelerations about the roll axis indicates that it is not due to a non-rigid body effect. It can also be seen that there is no frequency shift (the hump at 16.6 Hz in the error signal matches the hump in the load cell data at that frequency) so the error is not a nonlinear function of the modeled variables. The only remaining explanation is that the error is due to an unmodeled exteral load with predominant effect in the roll axis. A potential candidate for the source of this load is the drive train since it would affect only the roll moment. Measurements of the shaft torques from the engine and the tail rotor are required to verify this and could be used to compensate for this effect.

The unknown roll torque may be reconstructed from Eq. 1.3 to give further insight into its source. Fig. 18 is a plot of the phase of the unmodeled torque relative to the applied excitation as a function of frequency for four levels of applied y-axis load. It can be seen that the phase is sufficiently close to 180 degrees to indicate that the torque is due to elastic rather than damping effects. This is consistent with the possibility of a binding in the drive train rotation.

The pronounced x-axis force error from x-axis excitation (Fig. 12) is also too great to be explained by parameter errors, sensor errors or angular accelerations and no frequency shift is present between input and output, so the effect is not due to a nonlinearity. Again the only remaining explanation is an unmodeled external load. A potential candidate for this load source is possible binding of a translational coupling on the drive train that is designed to prevent transmission of x-axis loads from the rotor through the drive train to the fuselage. Measurements of the tension in the drive train shaft will be required to confirm this and to properly account for this effect in the model.

Out of eighteen estimates (six axes of estimates for each of three axes of applied loads) nominal parameter values produced estimation errors within the instrumentation noise level for all but two cases. Roll moment due to y-axis excitation and x-axis force due to x-axis excitation had errors too great to be explained by parameter uncertainties, so calibration is not needed to improve the accuracy in the other sixteen cases and would not help in these two cases. The source of these unknown loads must be determined and either be measured or modeled as a function of the measured loads before the model can be used to estimate roll moments and longitudinal forces.

Conclusions For Phase I

Concluding Remarks

An analytically derived model with nominal parameter values has been used to estimate applied rotor loads from measured load cell and accelerometer data. This approach has also provided a check on the consistency of the measured input output data. The presence of an unmodeled roll torque due to y-axis applied loads and an unmodeled x-force due to applied x-axis loads have been detected. Reconstruction of

the unmodeled loads shows that they have a phase lag close to 180 degrees from the applied load and are therefore predominantly elastic in nature. Rotational and translational binding in the drive train appears to be the most likely source of these unmodeled loads Shaft torsion and tension measurements will be required to confirm this and to incorporate these effects in the model

Specific Conclusions

The following conclusions are drawn from this study

An analytically derived linear, rigid body model of the isolated rotor/ transmission system with nominal parameter values provides estimates with errors within the level of the sensor noise for all cases but roll torque due to applied y-axis load and x-force due to applied x-axis load

Non-rigid body effects or nonlinear behavior can not explain the large errors present in these two cases The error must be due to an externally applied, unmodeled load The presence of such an unmodeled load could also account for the apparent nonlinearities detected by the previously attempted transfer function identification If there are unmodeled load sources the transfer functions will assume whatever values are required to reproduce the load cell readings given the measured loads If the unmodeled loads are elastic, and therefore dependent on the applied loads then different transfer functions will be identified at different applied loads This is precisely the effect observed in identifying transfer functions from the shake test data

Reconstruction of the unmodeled load from the error signal indicates it is predominantly elastic in nature If so, it was probably present in the static calibration and could account for the apparent nonlinearities detected in the static calibration Applying a regression fit to input/output data in the presence of an unknown input will result in the identified coefficients taking on whatever values are required to account for the unknown input. As in the shake test case, if the unknown loads are elastic, they will be dependent on the applied loads and the identified coefficients will vary with applied load This effect was observed in identifying a model from the static test data

Calibration of the parameters is unnecessary at this point since the design values appear to give satisfactory results when the external loads are all properly included.

Recommendation For Further Research

The following recommendations are made

If the unmodeled loads are elastic, rather than damping, as the phase lag appears to suggest, then these loads were probably present in the static test and could account for the apparent nonlinearity in that calibration The analytical model should be applied to the existing static calibration data to determine if the same unmodeled loads appear to have been present

The upcoming static calibration should be sufficiently instrumented to detect the suspected sources of unmodeled loads from the drive train and the analytical model should be used to process the data with sufficiently fast turn-around that newly identified effects can be investigated before the tests are completed

The approach should be applied to static test data to evaluate the calibration technique Nominal parameter values have done surprisingly well in allowing accurate hub load estimation for the specific static load condition present in the dynamic data Static test experience suggests that this will not be true under all static load conditions Once the model structure is fully validated it should be applied to static test data to determine which parameters to calibrate and to determine the range of variation of the parameters through calibration

PHASE II: IDENTIFICATION OF ROTOR/TRANSMISSION/LOAD CELL MODEL PARAMETERS DIRECTLY FROM FLIGHT TEST DATA

Background

Overview

Phase I of this study concentrated on the development of an analytical model of the rotor/transmission/load cell system and on the validation of that model from ground test data. It was determined that under some loading conditions, unmodeled external loads are present and these loads must be accounted for before the model can be further improved. Once this is accomplished, the next step will be to validate the model parameters over a range of operating conditions. The available data in Phase I tended to confirm that parameter values obtained from the design specifications were adequate but this set of data included only one static load condition and the parameters of the model are more likely to be dependent on the high magnitude static loads than on the lower magnitude dynamic loads. It is possible that the parameters will vary with flight condition and must therefore be calibrated against static load. If the dependency is a simple one, then this may be readily accomplished by ground based calibration. If the dependency is complicated, however, the required ground testing could be costly and the resulting calibration curve may be inaccurate over some regions of the operating regime.

Modern parameter identification techniques provide an alternative to laboratory calibration by allowing direct identification of the parameters from input, output data in the operational environment. This has the advantage that there is no need to characterize a complicated functional dependency in order to determine the parameter values. The parameters are identified that provide the best fit of the model to the input, output data over a specified data record. If the parameters vary slowly relative to the length of the data record, the identification may be more accurate than could be obtained from a calibration curve of limited order. The high cost of generating complicated calibration curves from ground testing is also eliminated.

Phase II of this study examines the use of modern parameter identification methods in identifying the parameters of the RSRA rotor transmission load cell model directly from available flight data. In order to facilitate the study, the data set was generated by a computer simulation using a model with the same structure assumed by the parameter identification method but with different parameter values. Since this approach only identifies parameters and does not question the model structure it can only be used with models whose structure has been adequately validated from ground tests.

Identification and Calibration

Identification methods can be classified into three categories.

1) *Equation Error Method.* In this method a set of measured inputs, u, and outputs y, are assumed related by a known mathematical model $f(u, y) = 0$ and the parameters of the model are identified by a least squares minimization of the equation error $f(u, y)$. This technique is commonly referred to as regression and requires accurate measurements of both the input and output.

2) *Output Error Method* In this method, the parameters of the assumed mathematical model are identified by a least squares minimization of the output error, determined as the difference between the output of the model of the system, and the output of the actual system 8 This approach also requires measurements of both inputs and outputs.

3) *Maximum Likelihood Method* In this method, a Kalman Filter is constructed using a dynamic system model and an algebraic sensor model The parameters of both models are then identified by a weighted least squares minimization of the output error of the Kalman Filter (innovations sequence) 8 . Note that if only the parameters of the sensor model are to be identified the Kalman Filter can be used to estimate the inputs to the sensor model therefore, only the sensor outputs need be measured This feature makes the Maximum Likelihood approach particularly relevant to sensor calibration in an operational environment

Calibration methods can be categorized based on the parameter identification technique used The following definitions are proposed

1) *Off-line Calibration.* This refers to calibration using either the Equation Error Method or the Output Error Method in a test environment where both the sensor input and output are known Once the sensor parameters have been identified, they are used with the sensor model in the operational environment to estimate the sensor input (system states) from measurements of the sensor output Since the parameters are not identified from data obtained in the operational environment, this method is referred to as "off-line calibration " This is the most commonly used approach to sensor calibration

2) *On-line Calibration* This method uses the Maximum Likelihood Method to estimate simultaneously the parameters of the sensor model and the input to the sensor (system states) Only the measured output of the sensor and a model of the dynamics of the system driving the sensor are needed Since no knowledge of the input is required, the parameter identifiction may be performed using data obtained in the actual operational environment hence the term "on-line calibration Note that "on-line", as used here, does not imply "real-time" Calibration by post-experiment data processing still fits the definition of on-line calibration

Off-line calibration is well suited to situations where the parameters are constant or simple functions of the environment Under these circumstances, it is the preferable approach because it provides a simple means of applying the identified parameters to the sensor model to estimate the states in an operational environment When the parameters of the sensor model become complicated functions of the system states, however, the off-line calibration procedure becomes more involved It is then necessary to relate the parameters to measurable quantities, such as the sensor output, through additional mathematical models (usually polynomials) the calibration then involves identifying the coefficients of these additional models

On-line calibration is ideally suited to handle situations where the sensor model parameters are complicated functions of time or the system states Since the parameters of the sensor model are directly identified in the actual operational environment, there is no need to further characterize the parameters as functions of measurable quantities Thus far, on-line calibration has been used principally in support of parameter identification of dynamic system models This paper will address on-line calibration as a technique for obtaining more accurate calibrations of sensor models with variable parameters

Objective And Approach

The objective of this study is to apply the on-line calibration method to the problem of calibrating the RSRA load cells The rationale is that by directly identifying variable parameters of the load cell model in the operating environment, the need to model their functional dependence on applied loads is eliminated and a more accurate estimate of the applied loads at the hub may be obtained The technique was evaluated by using computer simulations of the load cell response to applied loads to generate data for the on-line calibration algorithm The emphasis was on calibrating the load cells for high frequency applied loads (17 Hz), because a major objective of the RSRA program is to use the load cells to evaluate coupling of rotor loads at the N_b/revolution blade passage frequency (the number of blades, N_b , times the shaft rotational rate,) The simulation discussed here is necessary to refine the on-line method before committment to flight tests or other experiments.

Design Of The On-Line Calibration Algorithm

Approach

The design of the on-line calibration algorithm for the RSRA load cells includes the following steps

1) Define the load cell model In this step a mathematical model relating applied rotor loads to load cell readings and inertial loads for the isolated rotor transmission system is derived The model must be formulated so that its variation with applied loads can be represented by a set of identifiable parameters

2) Define a model of the dynamics of the applied rotor loads Since knowledge of the rotor load dynamics is used as an alternative to knowledge of the actual loads in on-line calibration, it is essential that an accurate representation of these dynamics be derived The derived model must have sufficient degrees of freedom to allow its transient response to be fit to the experimental data

3) Design a Kalman Filter to estimate the applied rotor loads The dynamic model of the rotor loads and the model of the load cell response to rotor loads are combined in a Kalman Filter to estimate the net applied loads at the rotor hub The accuracy of the estimate depends on the accuracy of the parameters in the load cell model

4) Design a Maximum Likelihood estimator for the parameters of the load cell model The Maximum Likelihood parameter identification algorithm uses the measurement error generated by the Kalman Filter to estimate the parameters of the load cell model The updated parameters are then used in the Kalman filter to obtain improved estimates of the applied rotor loads

The interaction of these four modules with measurements obtained from the aircraft is shown in Figure 19 The Kalman Filter consists of the dynamic model and the sensor model linked together by feedback loops with Kalman gains, K The function of the Kalman Filter is to generate an estimate, $\hat{H}$ of the system states, $\vec{H}$, using available measurements $\vec{T}$ and $\vec{J}$, to be described below These estimates are based on assumed values, $\vec{\Theta}$, for the parameters of the models, $\vec{\Theta}$ The Maximum Likelihood Method then uses a gradient algorithm on the sequence of Kalman Filter measurement errors , $\vec{e}_J$, to generate new

estimates, $\hat{\Theta}$ of the parameters of the models 8 . For purposes of this study, the RSRA measurements were simulated using computer models that were independent of the models used in the calibration algorithm The success of the algorithm was then determined by observing the convergence of the models in the calibration algorithm to the models in the RSRA-measurement simulation

The Load Cell Model

The load cell model used for this study is the model derived in Phase I and described in detail in Appendix A The parameter set to be identified will be limited to the load cell deformation angles for purposes of this study, although any of the geometric or mass properties parameters included in the derivation in Appendix A could be identified The parameters will be identified from the error between the measured inertial loads, as obtained from the accelerometers and mass properties, and the estimated inertial loads, as obtained from Eq 1 1 as a function of the parameter set and the applied rotor loads The model, as given by Eq 1.1, is therefore solved for the inertial loads, $\bar{J}$, to give an equation of the form

$$\bar{J} = -S(\bar{\alpha})\bar{T} - R\bar{H} - \bar{\nu}, \qquad \bar{\nu} = N(0, Q_\nu) \tag{2 1}$$

where $\bar{J}$ is the vector of the six components of inertial loads acting at the center of mass, $\bar{T}$ is a vector consisting of the seven resultant load cell loads, and $\bar{H}$ is a vector of the six components of applied loads at the rotor hub. The measurement noise vector, $\bar{\nu}$, is added to characterize the stochastic nature of the inertial loads measurement. The noise is assumed to be normally distributed with zero mean and power spectral density Q_ν The S matrix is a 6 x 7 geometric matrix that transforms the seven load cell resultant loads at the load cell attach points to a set of six component loads at the center of mass Note that this matrix is a function of the fourteen arbitrary load cell deformation angles $\bar{\alpha}$, that we will use as the parameter set to be identified The R matrix is a 6 x 6 geometric matrix that transforms the six components of applied loads at the hub to six components of applied loads at the center of mass of the rotor/transmission system A detailed description of these vectors and matrices is given in Appendix A

Equation 2 1 will be used as the sensor model, relating load cell measurements, $\bar{T}$ to applied rotor loads, $\bar{H}$ We have therefore derived a sensor model where the effects of fuselage deformations can be represented by the set of 14 load cell deformation angles Calibration of this model consists of identifying these angles Either off-line or on-line calibration techniques can be used to accomplish this, but since the angles are complicated functions of the applied rotor loads, an off-line calibration procedure would require modeling and calibrating this functional dependency The on-line calibration procedure allows direct identification of these angles in the operating environment in which they will be used to estimate the hub loads, consequently, there is no need to model their functional dependency on the applied loads

The assumptions used in the derivation of this model are

1) The rotor/transmission system is a rigid body, therefore, all changes in the load cell geometry are due to relative fuselage deformations This assumption allows the net effect of the fuselage deformation on the load cell geometry to be completely characterized by a set of two orthogonal rotations of the load cell axis about each attach point The relative geometry of the applied loads at the hub and inertial loads at the center of mass do not change

2) Applied loads at the load cell attach points are directed along the load cell axis and no moments are supported at the spherical bearings This essentially assumes no friction in the bearings and is contrary to experimental evidence A significant level of hysteresis has been observed due to bearing friction This effect can be incorporated into the model at a later time but will be neglected here for purposes of evaluating the on-line calibration procedure

A third assumption not inherent in the model but used in the on-line calibration algorithm, is that the load cell deformation angles vary slowly so they may be treated as constant parameters over the data sets used for identification

A Dynamic Model of the Applied Rotor Loads

A key element in on-line calibration is the use of a dynamic model of the system driving the sensors. It is this model, in connection with the time varying data record that allows calibration with specific knowledge of the sensor input. The application addressed here requires the modeling of the dynamics of the applied rotor loads since this is the input to the load cells Modeling the rotor load dynamics across all frequencies would be a formidable task, requiring accurate knowledge of the dynamic load response to pilot inputs and changing flight environment There are frequencies, however, at which the dynamics of the rotor loads are well known. In a rotorcraft, strong vibratory loads are present at the one/ revolution frequency and at the N_b /rev frequency and its harmonics, where N_b is the number of blades of the rotor (currently $N_b = 5$ for the RSRA) These vibratory loads may be modeled using second order systems with zero damping and resonant frequencies at the prescribed values By filtering the load cell and accelerometer data to pass only these frequencies, the dynamic content in the filtered data will be accurately represented by the specified models This dynamic content is essential to the identification of even quasistatic parameters since there are more parameters than equations and the problem is therefore statically indeterminate

By filtering the data to pass only selected frequencies with vibratory loads, the pilot input is eliminated from the data Pilot input is normally used in parameter identification to insure that the parameters are identifiable by providing sufficient degrees of freedom in the dynamic response and by exciting all modes of the dynamic system Since the parameters to be identified are all in the algebraic sensor model there are no specific modes to excite, but the input to the load cells must have at least as many degrees of freedom as there are parameters to be identified In this case there are fourteen unknown parameters If we model the vibration at one frequency as a second order system for each component of hub load, the dynamic response will contain 12 independent components (a sine and a cosine component for each of the six hub loads) We therefore need to pass two frequencies with vibratory loads so that the dynamics will contain 24 degrees of freedom and insure identifiability for the 14 parameters Using this approach makes the parameter identification process independent of the pilot input allowing the calibration to proceed in parallel with any chosen flight maneuver

Since two vibration frequencies must be passed for adequate sensor excitation, the two lowest frequency vibration modes associated with the rotor will be used These are the one rev and the N_b/rev frequencies The dynamic models for the one rev and the N_b/ rev vibrations are given by the following equations

$$\ddot{\vec{H}}_1 - \Omega^2 \vec{H}_1 = \vec{\eta}_1 \qquad \eta_1 = \mathcal{N}(0\ Q_{\eta_1}) \tag{2.2}$$

$$\ddot{\vec{H}}_N - (N_b\Omega)^2 \vec{H}_N = \vec{\eta}_N, \qquad \eta_N = \mathcal{N}(0, Q_{\eta_N}) \tag{2.3}$$

where Ω is the rotational frequency of the rotor and η_1 and η_2 are normally distributed random variables with zero mean and power spectral densities Q_{n_1} and Q_{n_2}, respectively. Both H_1 and H_2 are six component hub load vectors and the total hub load vector present in the filtered data is given by

$$\vec{H} = \vec{H}_1 - \vec{H}_2 \tag{2.4}$$

While Equations 2.2 through 2.4 are not physically based models of the vibratory loads, they provide a mathematical representation that can be used to fit the dynamic content of the filtered data. By specifically characterizing the frequency characteristics, a more accurate fit to the data can be obtained for a model of given order.

Equations 2.2 and 2.3 may be written in state variable form as

$$d/dt \begin{bmatrix} \vec{H}_1 \\ \dot{\vec{H}}_1 \\ \vec{H}_2 \\ \dot{\vec{H}}_2 \end{bmatrix} = \begin{bmatrix} 0 & I & 0 & 0 \\ -\Omega^2 I & 0 & 0 & 0 \\ 0 & 0 & 0 & I \\ 0 & 0 & -(N_b\Omega)^2 I & 0 \end{bmatrix} \begin{bmatrix} \vec{H}_1 \\ \dot{\vec{H}}_1 \\ \vec{H}_2 \\ \dot{\vec{H}}_2 \end{bmatrix} - \begin{bmatrix} 0 \\ \vec{n}_1 \\ 0 \\ \vec{n}_2 \end{bmatrix} \tag{2.5}$$

Defining a state vector, $\vec{x}$, by

$$\vec{x} = \begin{bmatrix} \vec{H}_1 & \dot{\vec{H}}_1 & \vec{H}_2 & \dot{\vec{H}}_2 \end{bmatrix}^T \tag{2.6}$$

we may write Equation 2.5 as

$$\dot{\vec{x}} = F\vec{x} - \vec{\eta}, \qquad \vec{\eta} = N(0, Q_n) \tag{2.7}$$

The value of $\vec{x}$ at time n, $\vec{x}(n)$, may then be computed from $\vec{x}(n-1)$ by

$$\vec{x}(n) = \Phi(\Delta t)\vec{x}(n-1) - \int_0^{\Delta t} \Phi(\Delta t - \tau)\eta(\tau)d\tau \tag{2.8}$$

where the time interval from $n-1$ to n is Δt and

$$\Phi(\Delta t) = e^{F\Delta t} \tag{2.9}$$

Design of the Kalman Filter

Having defined a dynamic model of the rotor loads and a geometric model of the response of the load cells to applied rotor loads and inertial loads, a Kalman Filter to estimate the rotor loads may be derived. The sensor model, Equation 2.1, will be used as the measurement equation but the load cell readings, $\vec{T}$, cannot be used as the measurements. This is because Kalman filter must estimate the measurements from its state estimates and use the error between the estimated and actual measurements to update the state estimates. There are seven load cells but only six measurement equations in Equation 2.1. As a result, a unique set of estimated load cell readings, $\vec{T}$, cannot be generated from the six state estimates using the six measurement equations. The solution to this problem is to use the inertial loads because they may be uniquely estimated from the six estimated rotor loads and the seven known load cell loads using the six measurement equations of Equation 2.1. It should be noted that the inertial loads cannot actually be directly measured but must be computed from available accelerometer measurements and assumed mass

properties The accuracy of the assumed mass properties and accelerometer responses could significantly affect the results

Equations 2 1, 2.4, and 2 6 may be combined and written in the form

$$\vec{J} = -S(\vec{\alpha})\vec{T} - R\,\vec{H}_1 - \vec{H}_2 = J(\vec{\alpha}.\vec{T},\vec{x}) \tag{2 10}$$

The Kalman Filter 5 may now be written using Equation 2 10 as the sensor model and Equation 2 7 as the dynamic model Between measurement updates the state estimates, $\vec{x}$, are propagated by the deterministic part of Equation 2 8 as

$$\dot{\vec{x}}^{-}(n) = \Phi\dot{\vec{x}}^{-}(n-1) \tag{2 11}$$

where the superscripts - and − refer to estimates before and after the measurement update at the specified time

The post-measurement estimates may then be obtained from apriori estimates at the measurement update time, n, by

$$\dot{\vec{x}}^{-}(n) = \dot{\vec{x}}^{-}(n) - K(n)\,\vec{J}_m(n) - \vec{J}(\vec{\alpha}.\vec{T}(n)\;\dot{\vec{x}}^{-}(n)) \tag{2 12}$$

where $\vec{J}_m$ is a vector of 6 inertial loads derived from measured accelerations Note that the stochastic part of the dynamic model, Equation 2 8, is simulated by the measurement error feedback in the Kalman Filter. Equation 2 12 The Kalman gains $K(n)$, are given by:

$$K(n) = P^{-}(n)J_x^T\,J_xPJ_x^T - Q_v \tag{2 13}$$

where

$$J_x = -\;R\;\;0\;\;R\;\;0 \tag{2 14}$$

$$P^{-}(n) = \Phi P^{-}(n-1)\Phi^T - Q_n \tag{2 15}$$

and

$$P^{-}(n) = I - K(n)J_x\,P^{-}(n) \tag{2 16}$$

P^{-} and P^{-} are the apriori and post measurement variables of the state estimation error, respectively

Since J_x is constant and K is independent of the identified parameters, $\vec{\alpha}$, Equations (2 13) through (2 16) will reach a steady state condition that is independent of the identification process The algorithms can be greatly simplified by using the resulting steady state value of the Kalman gains, K, in Equation 2 12, thereby eliminating the need to use Equations 2 13 through 2 16 The use of a steady state Kalman filter where the gain is independent of the parameters to be identified insures a globally stable Maximum Likelihood Identification Algorithm [9]

The Maximum Likelihood Estimation Algorithm

The accuracy with which the Kalman Filter can estimate the applied hub loads depends on the accuracy of the estimate of the load cell deformation angles $\vec{\alpha}$. In the proposed approach these values are updated on-line using Maximum Likelihood parameter estimation. The Maximum Likelihood estimation algorithms are derived by minimizing a weighted sum of the squares of the measurement error of the Kalman Filter. (the innovations sequence) with respect to the parameters over a data set of N_s samples. The cost function is defined as

$$V = 1/2 \sum_{n=1}^{N_s} \vec{e}_J(n)^T W^{-1} \vec{e}_J(n) \tag{2.17}$$

where

$$\vec{e}_J = \vec{J}_m - \vec{J}(\vec{\alpha}, \vec{T}, \hat{\vec{x}}^-) \tag{2.18}$$

and

$$W = 1/N_s \sum_{n=1}^{N_s} \vec{e}_J(n) e^T{}_J(n) \tag{2.19}$$

Denoting the apriori estimate of the vector $\vec{\alpha}$ by $\hat{\alpha}$, and the post-measurement estimate by $\hat{\alpha}$, the first partial of V with respect to the deformation angles is expanded about its value at $\hat{\alpha}$ to give

$$\frac{\partial V(\hat{\alpha})}{\partial \vec{\alpha}} = \frac{\partial V(\hat{\alpha})}{\partial \vec{\alpha}} + (\hat{\alpha} - \hat{\alpha}) \frac{\partial^2 V(\hat{\alpha})}{\partial \vec{\alpha}^2} \tag{2.20}$$

Setting the desired value at $\hat{\alpha}$ to zero corresponding to an extremum, gives

$$\hat{\alpha} = \hat{\alpha} - \left(\frac{\partial^2 V(\hat{\alpha})}{\partial \vec{\alpha}^2} \right)^{-1} \left(\frac{\partial V(\alpha)}{\partial \vec{\alpha}} \right)^T \tag{2.21}$$

Taking the first partial of V with respect to α gives

$$\frac{\partial V(\hat{\alpha})}{\partial \vec{\alpha}} = \sum_{n=1}^{N_s} \vec{e}_J(n, \hat{\alpha})^T W^{-1} \left(\frac{\partial \vec{e}_J(n, \hat{\alpha})}{\partial \vec{\alpha}} \right) \tag{2.22}$$

where

$$\frac{\partial \vec{e}_J(n, \hat{\alpha})}{\partial \vec{\alpha}} = -J_\alpha \left(\hat{\alpha}, \vec{T}, \hat{\vec{x}}^-(n, \hat{\alpha}) \right) - J_x \left(\frac{\partial \hat{\vec{x}}^-(n, \hat{\alpha})}{\partial \vec{\alpha}} \right) \tag{2.23}$$

The dynamic behavior of the partial derivatives of the apriori state estimates, $\hat{\vec{x}}^-$, with respect to the angles, $\vec{\alpha}$ is obtained from Equations (2.11) and (2.12) as

$$\frac{\partial \hat{\vec{x}}^-(n, \hat{\alpha})}{\partial \vec{\alpha}} = \Phi I - K J_x \left(\frac{\partial \hat{\vec{x}}^-(n-1, \hat{\alpha})}{\partial \vec{\alpha}} \right) - K J_\alpha(\hat{\alpha}, \vec{T}, \hat{\vec{x}}^-(n-1, \hat{\alpha})) \tag{2.24}$$

where

$$\frac{\partial \hat{\vec{x}}^{-}(0,\vec{\alpha})}{\partial \vec{\alpha}} = 0 \tag{2 25}$$

The partials of the estimated inertial loads with respect to the angles J_α, are given by

$$J_\alpha(\vec{\alpha}, \vec{T}, \hat{\vec{x}}^{-}(n\ \vec{\alpha})) = \begin{bmatrix} (J_1)_\alpha \\ \\ (J_j)\vec{\alpha} \\ \\ (J_6)_\alpha \end{bmatrix} \tag{2 26}$$

where

$$(J_j)_\alpha = -\sum_{i=1}^{\tilde{i}} \frac{\partial S_{ij}(\vec{\alpha})}{\partial \vec{\alpha}} \vec{T}_i(n) \tag{2 27}$$

The second partial, to first order, is then

$$\frac{\partial^2 V(\vec{\alpha})}{\partial^2 \vec{\alpha}} = \sum_{n=1}^{N_s} \left(\frac{\partial \vec{e}_J(n,\vec{\alpha})}{\partial \vec{\alpha}}\right)^T W^{-1} \frac{\partial \vec{e}_J(n,\vec{\alpha})}{\partial \vec{\alpha}} \tag{2 28}$$

The parameter estimates are obtained from Equations 2 21 through 2 28 using the measurement error sequence, $\vec{e}_J$, generated by the Kalman Filter

Operational Approach

The data is first filtered to pass only the two specified frequencies The Kalman Filter is then applied to the data and allowed to reach steady state before the Maximum Likelihood algorithm begins operating on the measurement errors generated by the Kalman Filter The reason for waiting is that the error in the initial rotor load estimate will bias the estimates of the load cell angles By waiting until the transient due to this initial error decays we can eliminate this source of bias without having to add the initial conditions to our set of parameters to be identified This delay is necessary only on the first data used for identification If subsequent data sets are contiguous, the initial estimate of the hub load can be set to the final estimate of the hub load on the previous data set and the initial error will be small The statistics of the process and measurement noise, Q_η and Q_ν, are chosen to generate steady state Kalman gains from Equations 2 13 through 2 16 that provides a high filter bandwidth (short time constant) compared to the frequencies of the vibrations being tracked [10]

The Kalman Filter designed for use in calibrating the load cells will estimate only the one/rev and N_b/rev components of the hub loads If the low frequency response is also desired, it is necessary to pass the unfiltered data through a Kalman Filter that utilizes the updated parameters An additional 6 degrees of freedom dynamic model must be included in this Kalman Filter to track the low frequency components of the hub loads This additional states can be modeled by the Weiner process

$$\vec{H}_0 = \vec{\eta}_0 \qquad\qquad \vec{\eta}_0 = \Lambda(0, Q_{\eta_0}) \tag{2 29}$$

and the total hub loads are then given by

$$\vec{H} = \vec{H}_0 - \vec{H}_1 - \vec{H}_N \tag{2.30}$$

Simulation Results

The algorithms were implemented as shown in Figure 19, and a computer simulation of the applied hub loads and the measured load cell response was used to generate simulated measurement data for the RSRA. Again the problem of having to generate seven unique load cell readings using the specified hub loads and inertial loads with the six measurement equations was encountered. For purposes of simulation, the problem was solved by adding a seventh constraint equation which essentially minimized the strain energy in the load cells. This approach yielded reasonable simulation values of load cell readings for the applied hub loads. The physical basis for this constraint equation was too questionable to allow it to be utilized in the identification algorithm, so it was only used to generate simulated data with which to validate the algorithm. The deformation angles in the load cell simulation were set to arbitrary constant values and a different set of values were used with the Kalman Filter to initiate the identification process. Values of zero degrees were used for the simulation and four degrees for the Kalman Filter.

No inertial loads were simulated for the test since this represents a worst case for the identification process. Any input to the system from the inertial loads would have added additional degrees of freedom to the input to the load cells and thereby improved the identifiability of the load cell angles. Note that the presence of such additional measurement inputs would reduce the required number of degrees of freedom in the vibration model.

As explained in the previous section the initial values of the hub loads and the load cell deformation angles were set differently in the simulation model and in the calibration algorithm to evaluate the ability of the algorithm to converge to the values used in the simulation. Transients resulting from the initial state error in the Kalman Filter estimate will bias the parameter estimates. In order to avoid this problem, the filter was allowed to reach a steady state condition before the Maximum Likelihood algorithm was initiated.

The time constants chosen for the Kalman Filter were all at 0.1 seconds so a delay of about 0.5 seconds was necessary to insure that the response had reached a steady state condition. Two frequencies, one rev and N_b/rev, were included in the simulated hub load dynamics driving the load cell simulation. This was to insure that the load cell input had sufficient degrees of freedom to permit identification of the 14 load cell angles. It also effectively simulated filtering all but those frequencies in real test data. A sampling rate of 36 samples/second was used to insure adequate reconstruction of the 17 Hz, N_b revolution frequency.

Figure 20 is a plot of the error in the estimate of the longitudinal deformation angle of one of the vertical load cells. A delay of seventy samples in implementing the identification was used to allow the filter to reach steady state. A sequence of 10 samples was then used to perform the estimation. Due to the nonlinear nature of the measurement equation, multiple iterations over a data set were required to obtain convergence for the parameter estimates. On each iteration the seventy sample delay was repeated and the last 10 samples were used to estimate the load cell angles. Excellent convergence was obtained within four iterations over the same data set. Figure 21 is a similar plot for a lateral load cell deformation angle.

Figure 22 compares the actual y-axis hub load with estimates obtained using the initial and final parameter estimates. The estimates were obtained from a Kalman Filter with a Weiner process model of the additional low frequency states. The Kalman Filter used a simulated unfiltered data set that contained

a low frequency component in addition to the two vibratory components The hub load estimation error is significant for the initial parameter estimates but is considerably improved when the final parameter estimates are used A similar result is seen in Figure 23 for the applied roll moment at the hub The computer simulation demonstrates clearly the potential for performing on-line calibration of the load cells, using data obtained in the flight environment to simultaneously calibrate the load cells and estimate the hub loads Figures 22 and 23 demonstrate the sensitivity of the load estimation to errors in the load cell angles The load estimation error is significantly reduced when acurate estimates of the parameters are used

Identification From Ambient Vibrations

The demonstrated capability to identify parameters from ambient vibrations is significant in that it allows identification to proceed in an operational environment without the need to superimpose specially designed input signals to facilitate the identification The method may be applied to other problems beyond that discussed here For any such application the conditions for implementing this approach are as follows.

1) All parameters to be identified must be included in an algebraic representation of the system since dynamic models would require excitation at specific frequencies This does not present a problem since any dynamic model can be treated as a set of algebraic equations if all states and their derivatives are explicitly measured or estimated at each point in time

2) Ambient vibrations must include as many degrees of freedom as there are parameters to be identified and the dynamic model of the vibrations must also include these degrees of freedom This can be accomplished by modeling only the required number of degrees of freedom and filtering the data to pass only the modeled frequencies

Potential applications of this approach include the tracking of time varying stability derivatives of a flight vehicle during maneuvers that were designed to investigate performance This would provide a direct correlation between design parameters and observed handling qualities A real-time implementation of this identification technique would also facilitate adaptive control applications.

Conclusions For Phase II

Concluding Remarks

The purpose of Phase II of this study was to analytically demonstrate the feasibility of an on-line calibration procedure Rather than use experimental data, the investigation was conducted using data generated by a computer simulation of the load cells to allow a comparison of the identified model with the known simulation model The structure of the model to be identified, as implemented in the Kalman Filter, was the same as that used to generate the simulated load cell data, but the states and parameters of the two models were initialized differently The unknown model parameters (load cell deformation angles) were then identified successfully by applying the algorithm to the simulated load cell data The resulting estimate of the states (applied rotor loads) also converged to the values generated by the simulation. The model structure assumed for this investigation has not been validated with experimental data and the effect of using a model structure in the Kalman Filter that does not match the simulation model has not been investigated

Specific Conclusions

The following conclusions can be drawn

1) For the assumed model, the dynamic rotor-load estimates were found to be very sensitive to static load cell geometry deformations The rotor-load estimates were greatly improved by using identified geometric parameters

2) Calibration of all model parameters was successfully accomplished using only measured load cell and inertial loads data

3) The identification of the model parameters was accomplished using only rotor vibrations at the two lowest frequencies (one rev and N$_b$/rev) as the source of excita- tion. No specially designed external inputs were required

4) The identification was accomplished with the inertial load data set to zero This represents a worst case situation since any independent degrees of freedom in the inertial loads would provide excitation that would enhance the identification

Recommendation For Further Research

The following simulation-based investigations will be necessary to fully qualify the on-line calibration procedure for application to flight data

1) The capability to track time-varying deformation angles must be tested using simulated load cell data

2) The effect of sensor noise and model structure error on the identification must be determined

3) The effects on performance of varying the modeled vibration frequencies, the sampling rates and the Kalman Filter time constants should be investigated

A practical implementation of this methodology will require a validated mathematical model of the load cell response to applied rotor loads The accuracy of this technique is also dependent on the accuracies of the assumed mass properties and accelerometer responses. All of this must be determined from suitable ground tests before the on-line calibration approach can be applied to flight data

REFERENCES

1) Burks, J S , "*Rotor Systems Research Aircraft (RSRA) Rotor Force And Moment Measurement System*", AIAA First Flight Test Conference Las Vegas, Nev , Nov 1981

2) Acree C W , "*Results of the First Complete Static Calibration of the RSRA Rotor Load Measurement System* " NASA TP-2327, 1984

3) Wellman, B , "*Preliminary Results of the RSRA Shake Test*", To be published as a NASA TM 1985

4) Giansante, N Berman A Flannely W G and Nagy E J , "*Structural System Identification Technology Verification*", USAAVRADCOM Report No TR-81-D-28, Nov 1981

5) Bryson, A E , Jr and Ho, Y C . *Applied Optimal Control*. Blaisdell Publishing Co . Waltham Mass , 1969

6) Du Val. R W ."*The Use of Frequency Methods in Rotorcraft System Identification*". Paper No AIAA-81-2386. AIAA 1st Flight Testing Conference, Las Vegas. Nev . Nov , 1981

7) Jennrich. R E . Stepwise Regression.*Statistical Methods for Digital Computers*, Chapter 4. Wiley, New York

8) Mehra R K ,"*An Innovations Approach to Maximum Likelihood Identification of Linear and Non-linear Dynamic Systems*". Presented at the 5th Hawaii International Conference on System Science. 1972

9) Ljung L ."*Assympototic Behavior of the Extended Kalman Filter as a Parameter Estimator for Linear Systems*". IEEE Transactions on Automatic Control. Vol AC-24. No. 1. Feb . 1979

10) Bryson A E . Jr . and Hall, W Earl, Jr ."*Optimal Control and Filter Synthesis by Eigenvector Decomposition*". Report No 436. Dept of Aeronautics and Astronautics. Stanford University, Stanford CA . No . 1971

APPENDIX A: LOAD CELL MODEL DERIVATION

A diagram of the undeformed load cell geometry is shown in Figure A 1. The load cells are mounted to the fuselage and to the transmission base by spherical bearings It is assumed that the transmission base does not warp so all changes in the load cell geometry are due to deformations in the load cells themselves or in the fuselage mounting points With this assumption it is possible to completely model the load cell response using a general three component representation of the reaction force at each attach point on the transmission base, no knowledge of the fuselage deformation is required

Three plane views of the load cell geometry with the three component reaction force representation are shown in Figure A 2 Inertial loads including gravity and the drive shaft torque, are assumed to be concentrated at the transmission center of gravity The rotor loads are concentrated at the hub Taking the sum of the forces and moments about the center of gravity gives

$$
\begin{aligned}
X_c &= X_I - X_H - G_x - E_x - F_x - A_x - B_x - C_x - D_x = 0 \\
Y_c &= Y_I - Y_H - G_y - E_y - F_y - A_y - B_y - C_y - D_y = 0 \\
Z_c &= Z_I - Z_H - G_z - E_z - F_z - A_z - B_z - C_z - D_z = 0 \qquad (A\,1) \\
L_c &= L_I - L_H - Y_H hz - (A_z - D_z)w/2 - E_z e - (B_z - C_z)w/2 - F_z f \\
&\quad -(B_y - C_y - F_y - G_y - E_y - A_y - D_y)bz = 0 \\
M_c &= M_I - M_H - X_H hz - Z_H hx - (B_x - A_x - E_x - G_x)(d - \ell) - (C_x - D_x - F_x - B_x - A_x - E_x - G_x)bz \\
&\quad -(C_x - D_x - F_x)\ell = 0 \\
N_c &= N_I - N_H - (A_y - E_y - G_y - B_y)(d - \ell) - (C_y - F_y - D_y)\ell \\
&\quad -(A_x - D_x)w/2 - E_x e - (C_x - B_x)w/2 - F_x f = 0
\end{aligned}
$$

Using the transformations.

$$
\begin{aligned}
A_x &= A\cos(o_a)\sin(\theta_a) \\
A_y &= -A\sin(o_a)\cos(\theta_a) \\
A_z &= A\cos(o_a)\cos(\theta_a) \\
B_x &= B\cos(o_b)\sin(\theta_b) \\
B_y &= -B\sin(o_b) \qquad (A\,2) \\
B_z &= B\cos(o_b)\cos(\theta_b) \\
C_x &= C\cos(o_c)\sin(\theta_c) \\
C_y &= -C\sin(o_c) \\
C_z &= C\cos(o_c)\cos(\theta_c) \\
D_x &= D\cos(o_d)\sin(\theta_d) \\
D_y &= -D\sin(o_d) \\
D_z &= D\cos(o_d)\cos(\theta_d)
\end{aligned}
$$

$$E_x = -E\cos(o_e)\sin(\upsilon_e)$$
$$E_y = E\cos(o_e)\cos(\upsilon_e)$$
$$E_z = E\sin(o_e)$$
$$F_x = -F\cos(o_f)\sin(\upsilon_f)$$
$$F_y = F\cos(o_f)\cos(\upsilon_f)$$
$$F_z = F\sin(o_f)$$
$$G_x = G\cos(\theta_j)\cos(\upsilon_j)$$
$$G_y = G\cos(\theta_j)\sin(\upsilon_j)$$
$$G_z = -G\sin(\theta_j)$$

the equations become

$$\vec{J} - R\vec{H} - S\vec{T} = 0 \tag{A 3}$$

where

$$\vec{J}^T = X_I, Y_I, Z_I, L_I, M_I, N_I \tag{A 4}$$

and

$$\begin{bmatrix} X_I \\ Y_I \\ Z_I \\ L_I \\ M_I \\ N_I \end{bmatrix} = \begin{bmatrix} -m_x a_x \\ -m_y a_y - \Gamma_y q \\ -m_z a_z \\ -I_x p - Q_t - \Gamma_L q \\ -I_y q - \Gamma_M q \\ -I_z r \end{bmatrix} \tag{A 5}$$

In equation A 5, a_x, ay , and a_z are linear accelerations in each direction measured at the rotor/ transmission system center of gravity and p q and r are rotational accelerations Because of the nonrigid engine mountings the engine contributions to inertial forces are not equal in all directions when measured at the system center of gravity This effect can be adequately modeled by assigning different values to the total effective mass of the combined rotor transmission engine system in each direction. m_x, m_y, and m_z There are also a few minor error terms not given here that are discussed fully in Reference 4 I_x, I_y, and I_z are moments of inertia, related terms in the cross-products of rotational rates are neglible Q_t is total applied engine and tail rotor shaft torque Gyroscopic coupling forces due to engine and transmission rotational moments of momentum are represented by the coefficients Γ, with subscripts for the appropriate axis

The hub forces ($\vec{H}$) and load cell readings ($\vec{T}$) in Eq A 3 are given by

$$\vec{H} = X_H\ Y_H, Z_H, L_H, M_H, N_H \tag{A 6}$$
$$\vec{T} = A, B, C, D\ E, F, G \tag{A 7}$$

The geometric transformations from the applied loads to the center of mass (R and S) are given by

$$R = \begin{bmatrix} 1 & 0 & 0 & 0 & 0 & 0 \\ 0 & 1 & 0 & 0 & 0 & 0 \\ 0 & 0 & 1 & 0 & 0 & 0 \\ 0 & hz & 0 & 1 & 0 & 0 \\ -hz & 0 & hz & 0 & 1 & 0 \\ 0 & 0 & 0 & 0 & 0 & 1 \end{bmatrix} \tag{A 8}$$

and equation (A 9) (on the next page) in which C and S denote cosine and sine functions, respectively

$$
S = \begin{bmatrix}
C\phi_a S\theta_a & C\phi_a S\theta_b & C\phi_a S\theta_c & C\phi_a S\theta_d & C\phi_a S\psi_e & C\phi_a S\psi_f & C\phi_a S\psi_g \\
S\phi_a & S\phi_b & S\phi_c & S\phi_d & C\phi_e C\psi_e & C\phi_f C\psi_f & -C\theta_g S\psi_g \\
C\phi_a C\theta_a & C\phi_b C\theta_b & C\phi_c C\theta_c & C\phi_d C\theta_d & S\phi_e & S\phi_f & S\theta_g \\
\frac{a}{2} C\phi_a C\theta_a + b z S\phi_a & b z S\phi_b + \frac{a}{2} C\phi_b C\theta_b & b z S\phi_c + \frac{a}{2} C\phi_c C\theta_c & b z S\phi_d + \frac{a}{2} C\phi_d C\theta_d & e S\phi_e - b z C\phi_e C\psi_e & - f S\phi_f + b z C\phi_f C\psi_f & b z C\theta_g S\psi_g \\
b z C\phi_a S\theta_a + (d - f) C\phi_a C\theta_a & b z C\phi_b S\theta_b + (d - f) C\phi_b C\theta_b & b z C\phi_c S\theta_c + (d - f) C\phi_c C\theta_c & b z C\phi_d S\theta_d + (d - f) C\phi_d C\theta_d & - b z C\phi_e S\psi_e + (d - f) S\phi_e & b z C\phi_f S\psi_f + f S\phi_f & b z C\theta_g C\psi_g + (d - f) S\theta_g \\
\frac{a}{2} C\phi_a C\theta_a + (d - f) S\phi_a & \frac{a}{2} C\phi_b C\theta_b + (d - f) S\phi_b & f S\phi_c + \frac{a}{2} C\phi_c C\theta_c & f S\phi_d + \frac{a}{2} C\phi_d C\theta_d & a C\phi_e S\psi_e + (d - f) C\phi_e C\psi_e & - f C\phi_f C\psi_f + f C\phi_f S\psi_f & (d - f) C\theta_g S\psi_g
\end{bmatrix} \tag{A9}
$$

APPENDIX B: THE EFFECT OF SENSOR NOISE ON LOAD ESTIMATION

The analytical model of the rotor/transmission system derived in the text has the form

$$\vec{J} - S\vec{T} - R\vec{H} = 0 \qquad (B.1)$$

Given the measured load cell readings, $\vec{T}_m$, and inertial loads derived from accelerometer measurements $\vec{J}_m$, the applied rotor loads, $\vec{H}$, are estimated from Eq. B 1 as

$$\hat{\vec{H}} = -R^{-1}\vec{J}_m - S\vec{T}_m \qquad (B\,2)$$

The measured load cell and accelerometer values may be written in terms of their true values and a random measurement noise component as follows

$$\vec{a}_m = a - \vec{\nu}_A, \qquad \vec{\nu}_A = N(0, Q_A) \qquad (B\,3)$$

$$\vec{T}_m = \vec{T} - \vec{\nu}_t, \qquad \vec{\nu}_T = N(0, Q_T) \qquad (B\,4)$$

Writing the derived inertial load vector, $\vec{J}_m$, as the product of an inertia matrix, M, and the accelerometer measurements a_m, gives

$$\vec{J}_m = M\vec{a}_m = M\vec{a} - M\vec{\nu}_A = \vec{J} - M\vec{\nu}_A \qquad (B\,5)$$

where $\vec{J}$ is the actual inertial load vector

Substituting Eq's B 4 and B 5 into Eq B 2 gives

$$\hat{\vec{H}} = -R^{-1}(\vec{J} - S\vec{T}) - \vec{\nu}_H \qquad (B\,6)$$

where

$$\vec{\nu}_H = -R^{-1}M\vec{\nu}_A - S\vec{\nu}_T \qquad (B\,7)$$

Substituting Eq B 1 into Eq B 6 then gives

$$\hat{\vec{H}} = \vec{H} - \vec{\nu}_H \qquad \vec{\nu}_H = N(0\ Q_H) \qquad (B\,8)$$

From Eq B 8 it is seen that $\vec{\nu}_H$, as given by Eq (B 7) is the combined effect of the instrumentation errors on the applied rotor load estimate, $\hat{\vec{H}}$ This error represents a lower bound on the accuracy of the estimation that is attainable without applying statistical processing, such as Kalman filtering or smoothing The covariance of this error, Q_H , may be computed from Eq (B 7) using the known covariance of the instrumentation errors, Q_A and Q_T , as follows

$$Q_H = E\{\vec{\nu}_H\vec{\nu}_H^T\} = E\{ -R^{-1}M\vec{\nu}_A - S\vec{\nu}_T, \\ -R^{-1}M\vec{\nu}_A - S\vec{\nu}_T{}^T \} \qquad (B\,9)$$

$$Q_H = R^{-1}ME\{\vec{\nu}_A\vec{\nu}_A^T\}M^T(R^{-1})^T - SE\{\vec{\nu}_T\vec{\nu}_A^T\}M^TR^{-1T} \\ - R^{-1}ME\{\vec{\nu}_A\vec{\nu}_T^T\}S^T(R^{-1})' - R^{-1}SE\{\vec{\nu}_T\vec{\nu}_T^T\}S'R^{-1} \qquad (B\,10)$$

The sensor noise components are assumed independent so the term $E\{\nu_A\nu_T{}^T\}$ is zero Substituting the known covariance matrices of the sensors for the other expected value terms gives

$$Q_H = R^{-1}MQ_AM^T - SQ_TS^T(R^{-1})^T \qquad (B\,11)$$

APPENDIX C: CALIBRATION ALGORITHM

The applied rotor load estimation error is given by Eq 1 3 in the text as

$$\vec{\epsilon}_H = -R^{-1}[\vec{J}_m - S\vec{T}_m - R\vec{H}] \tag{C 1}$$

The coefficient matrices, R and S contain geometric parameters of the model and the derived inertial loads vector, $\vec{J}_m$, includes inertial parameters of the model A subset, Θ, of the parameters is selected for calibration and the error is treated as a function of those parameters A cost function is written in the form

$$V(\Theta) = 1/2 \sum_{n=1}^{N_s} \vec{\epsilon}_H(\Theta, n)^T W^{-1} \vec{\epsilon}_H(\Theta, n) \tag{C 2}$$

where W is a weighting matrix given by

$$W = 1/N_s \sum_{n=1}^{N_s} \vec{\epsilon}_H(\Theta, n) \vec{\epsilon}_H(\Theta, n)^T \tag{C 3}$$

Denoting the apriori estimate of the vector $\vec{\Theta}$ by $\hat{\Theta}$ and the postmeasurement estimate by $\dot{\Theta}$, the first partial of V with respect to the parameter $\vec{\theta}$ is expanded about its value at the apriori parameter estimate $\hat{\Theta}$ to give

$$\frac{\partial V(\dot{\Theta})}{\partial \vec{\Theta}} = \frac{\partial V(\hat{\Theta})}{\partial \vec{\Theta}} - (\dot{\Theta} - \hat{\Theta}) \frac{\partial^2 V(\hat{\Theta})}{\partial^2 \vec{\Theta}} \tag{C 4}$$

Setting the desired value at $\dot{\Theta}$ to zero, corresponding to an extremum, gives

$$\dot{\Theta} = \hat{\Theta} - \left[\frac{\partial^2 V(\hat{\Theta})}{\partial \vec{\Theta}^2}\right]^{-1} \frac{\partial V(\hat{\Theta})}{\partial \vec{\Theta}}^T \tag{C.5}$$

Taking the first partial of V with respect to $\vec{\Theta}$ at $\hat{\Theta}$ gives

$$\frac{\partial V(\hat{\Theta})}{\partial \vec{\Theta}} = \sum_{n=1}^{N_s} \vec{\epsilon}_H(\hat{\Theta}, n)^T W^{-1} \frac{\partial \vec{\epsilon}_H(\hat{\Theta}, n)}{\partial \vec{\Theta}} \tag{C 6}$$

The second partial to first order is then

$$\frac{\partial^2 V(\hat{\Theta})}{\partial \vec{\Theta}^2} = \sum_{n=1}^{N_s} \left(\frac{\partial \vec{\epsilon}_H(\hat{\Theta}, n)}{\partial \vec{\Theta}}\right)^T W^{-1} \frac{\partial \vec{\epsilon}_H(\hat{\Theta}, n)}{\partial \vec{\Theta}} \tag{C 7}$$

Once the parameter set has been chosen, the partial derivative of the errors, $\vec{\epsilon}_H$, with respect to the parameters must be generated analytically from Eq (C 1) The parameter estimates are then obtained from Eqs (C 5) to (C 7) using the measurement errors sequence, $\vec{\epsilon}_H$ generated by Eq (C 1)

FIGURES

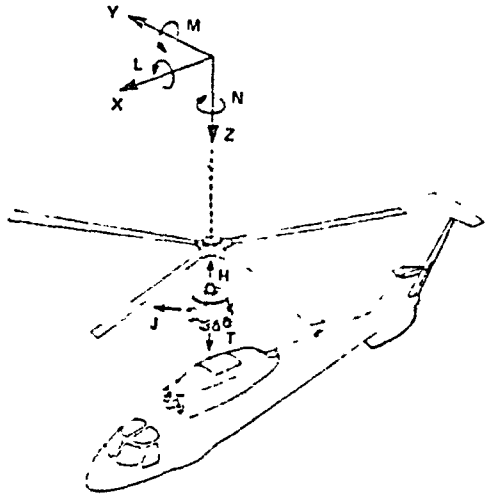

Figure 1 Loads acting on isolated Rotor 'Transmission

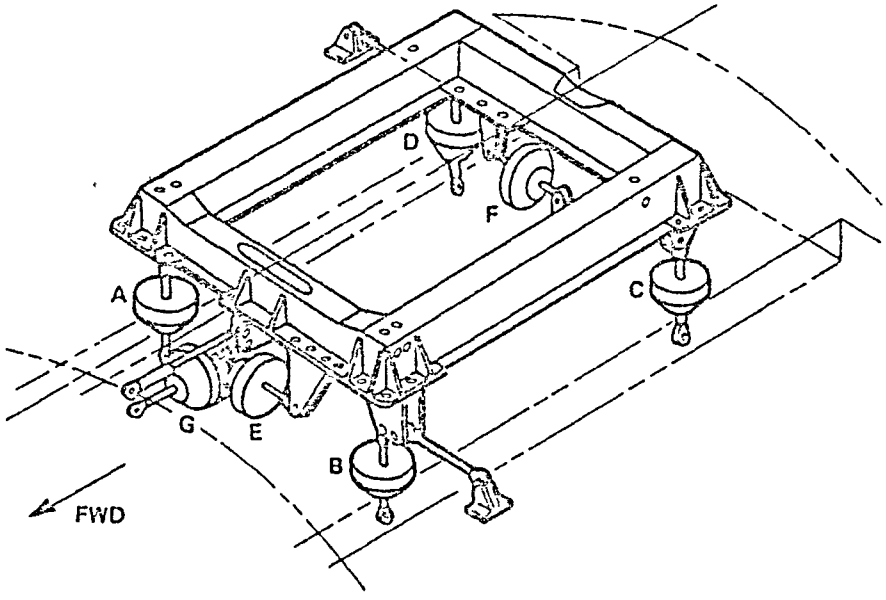

Figure 2 Load cell arrangement for Rotor 'Transmission System

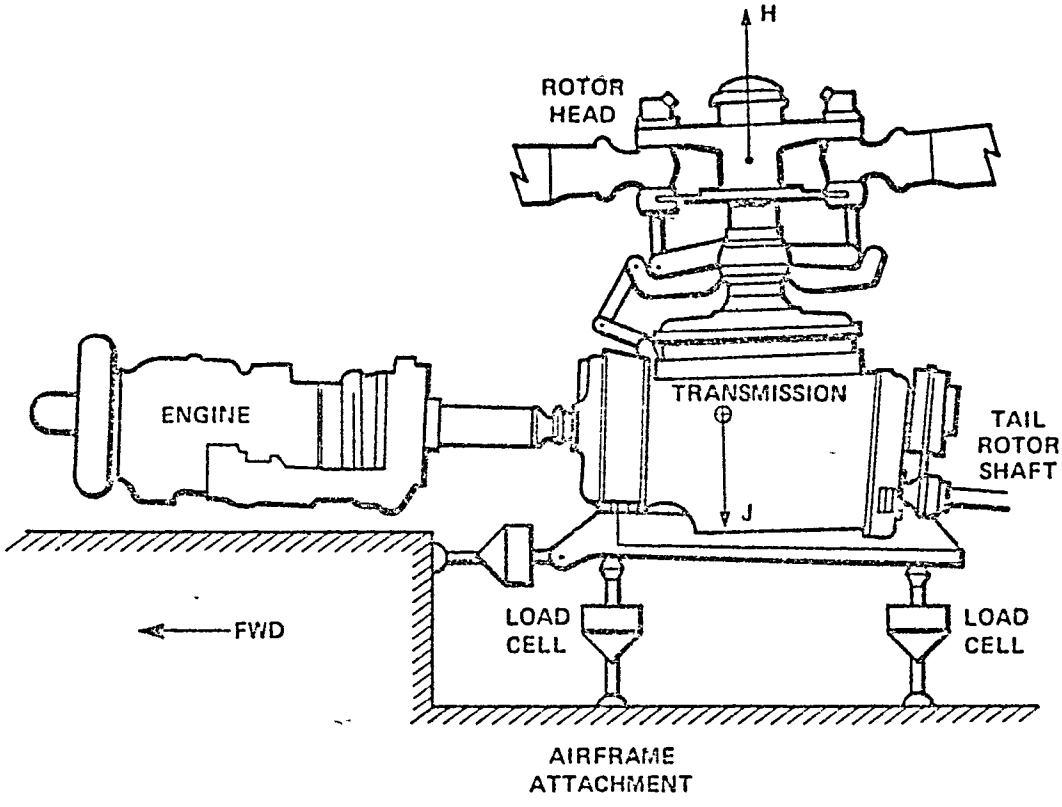

Figure 3 RSRA rotor balance system and mounted items

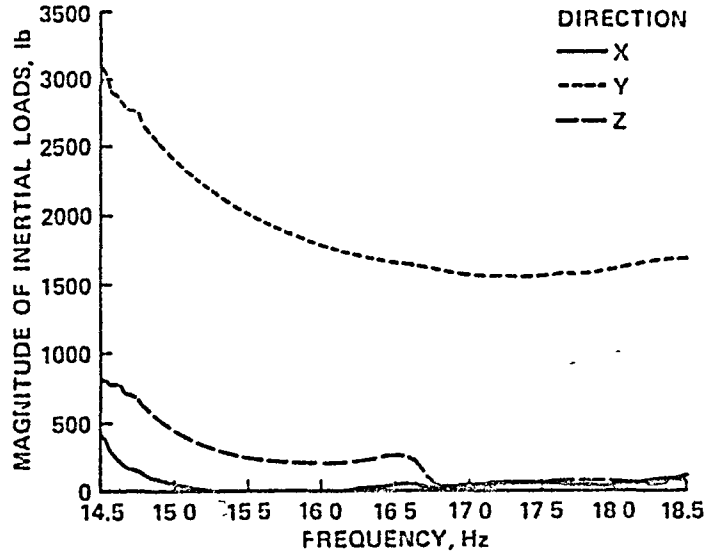

Figure 4 Magnitude of load cell transfer functions for 800 lb applied lateral force

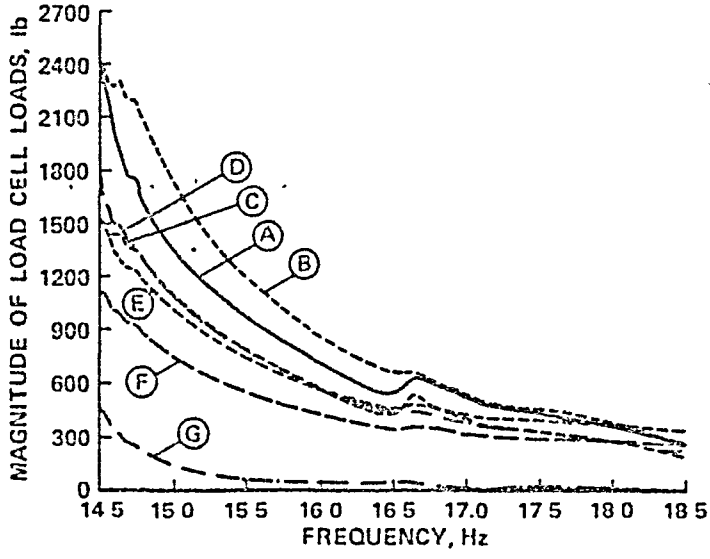

Figure 5 Magnitude of inertial load transfer functions for 800 lb applied lateral force

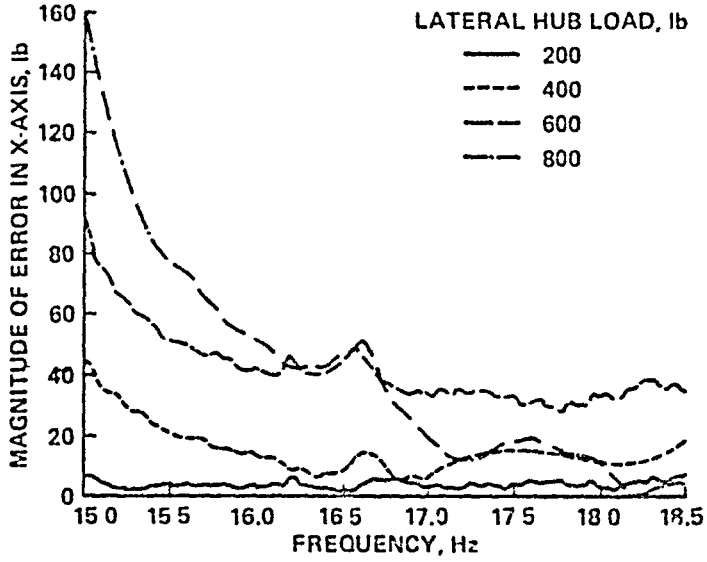

Figure 6 Magnitude of x-axis applied force estimation error for applied lateral forces

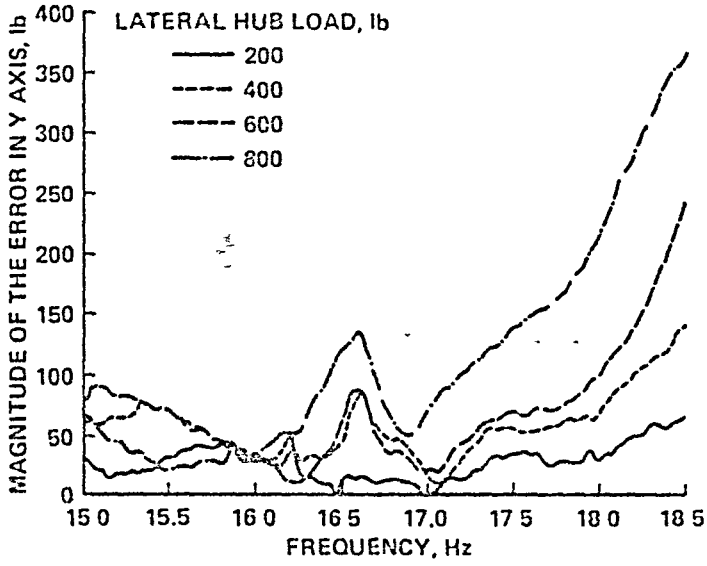

Figure 7 Magnitude of y-axis applied force estimation error for applied lateral forces

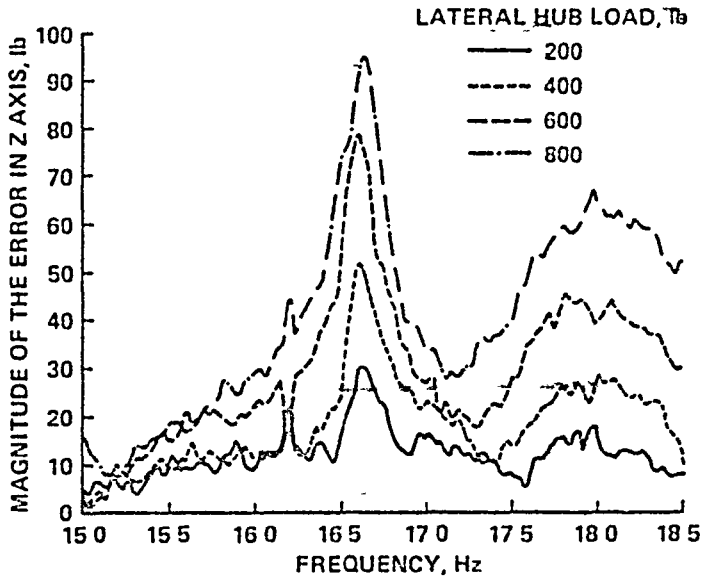

Figure 8 Magnitude of z-axis applied force estimation error for applied lateral forces

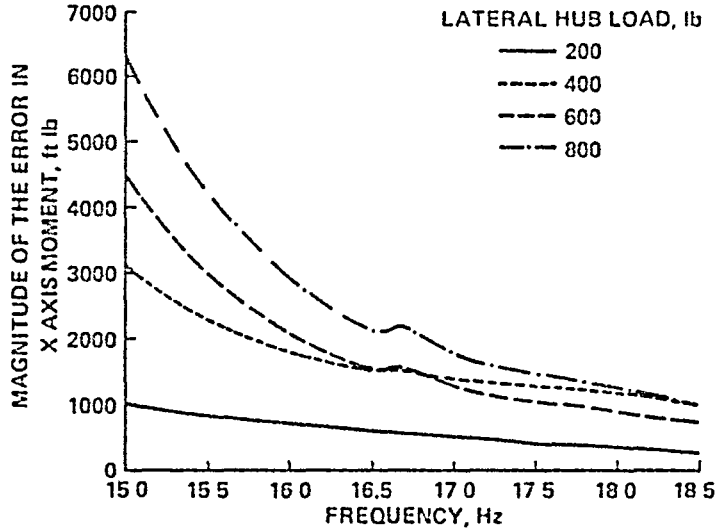

Figure 9 Magnitude of x-axis applied momert estimation error for applied lateral forces

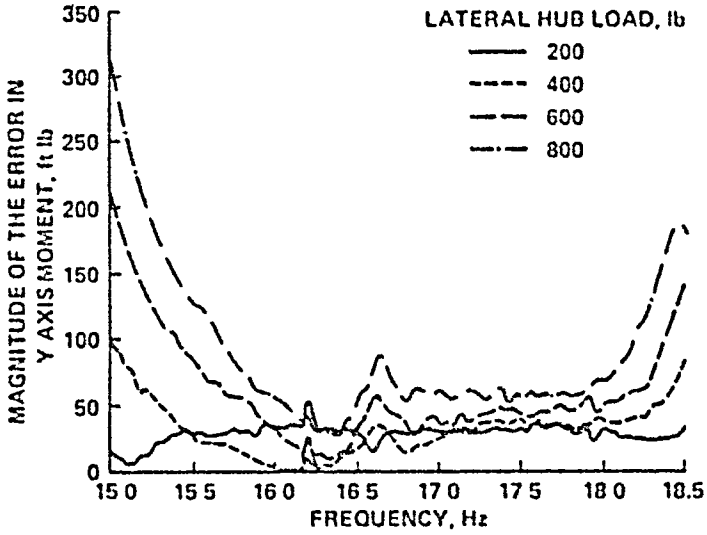

Figure 10 Magnitude of y-axis applied moment estimation error for applied lateral forces

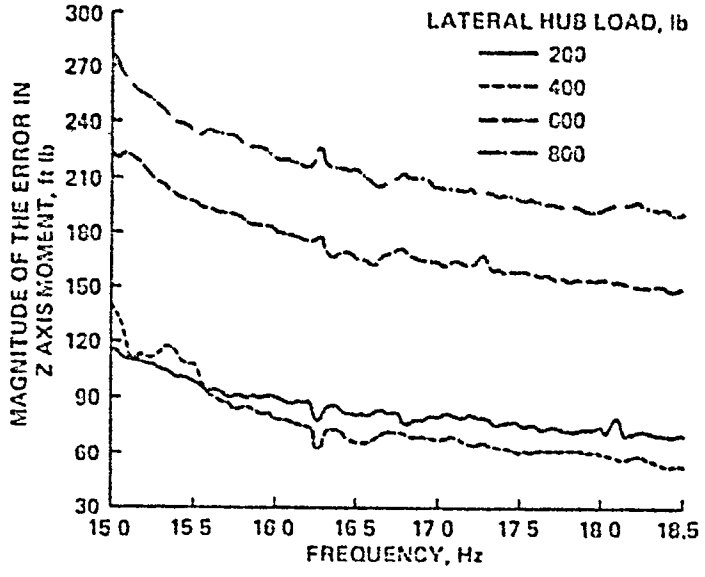

Figure 11 Magnitude of z-axis force estimation for applied x y and z axis loads

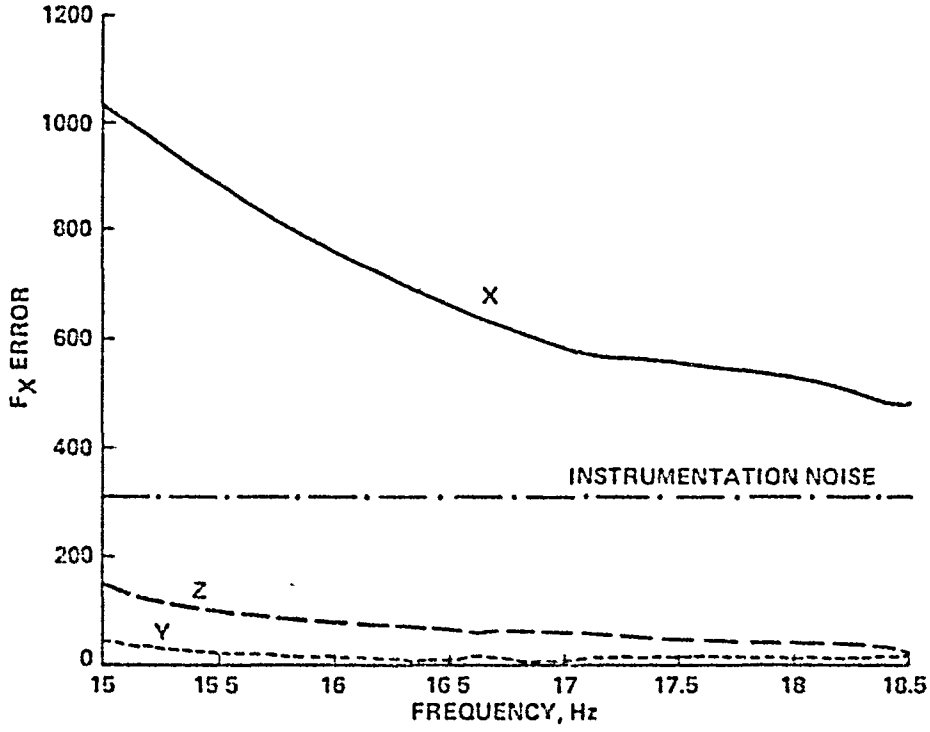

Figure 12 · Comparison of magnitudes of x-axis force estimation error for applied x, y and z-axis loads

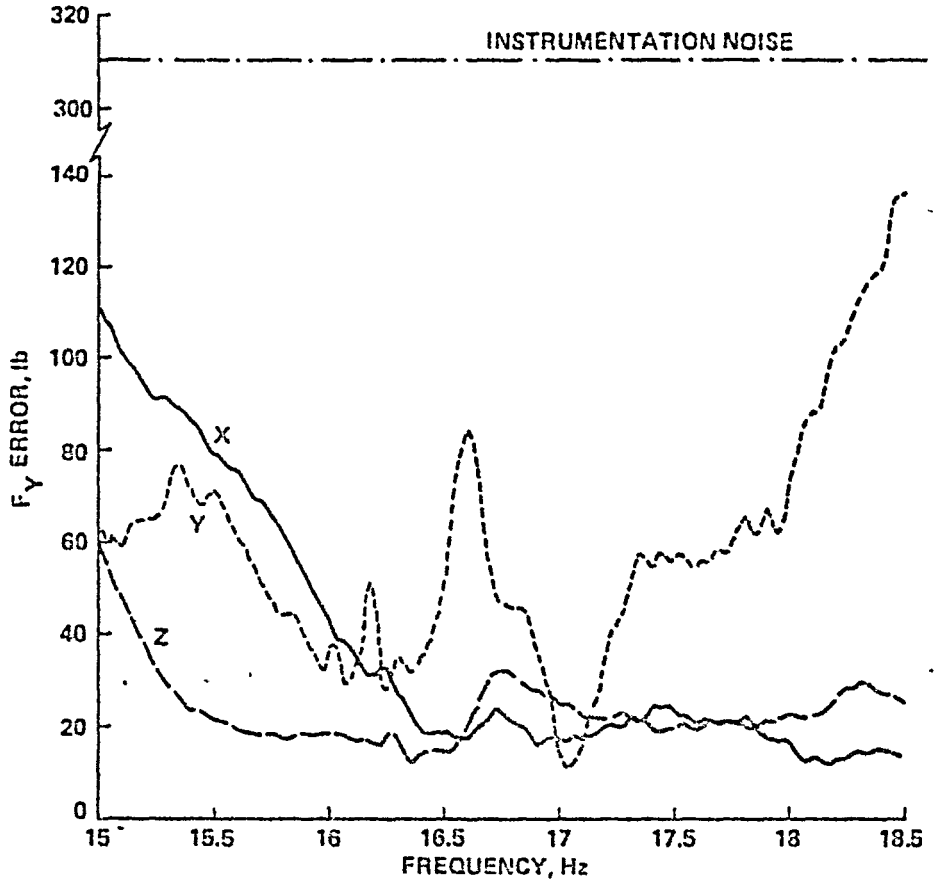

Figure 13 . Comparison of magnitude of the y-axis force estimation error for applied x, y and z axis loads.

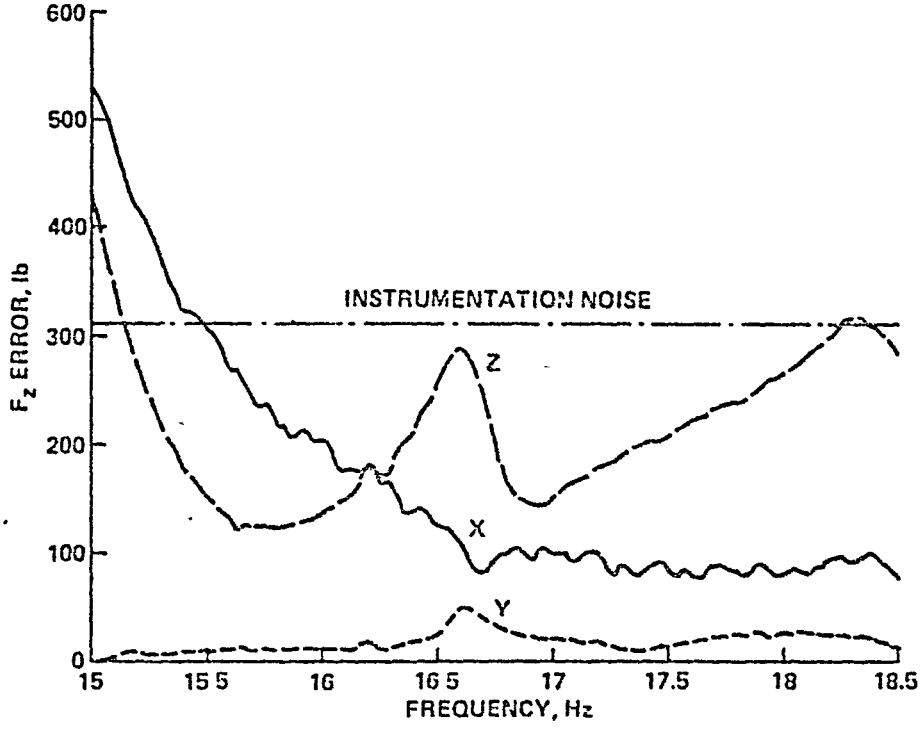

Figure 14 Comparison of magnitude of z-axis force estimation error for applied x, y and z axis loads

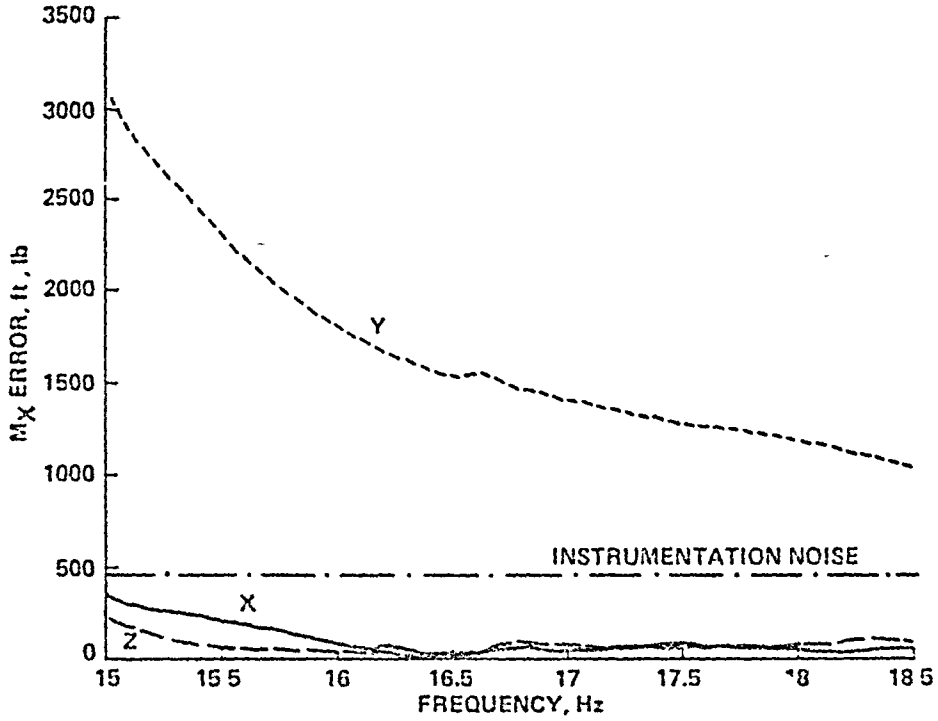

Figure 15 Comparison of magnitude of x-axis moment estimation error for applied x, y and z-axis

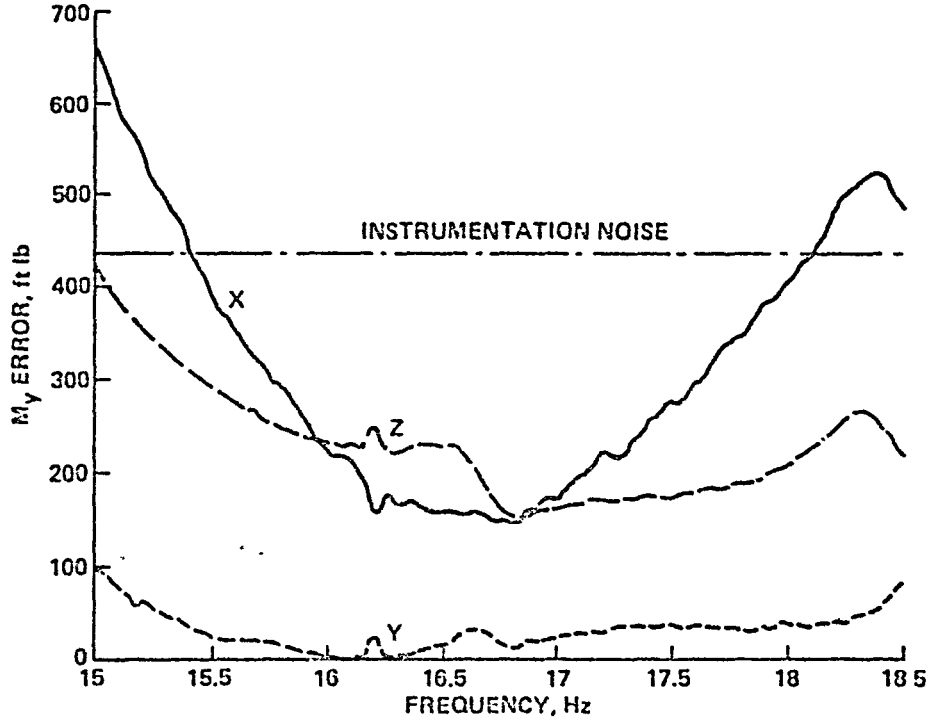

Figure 16 Comparison of magnitude of y-axis moment estimation error applied x, y and z-axis

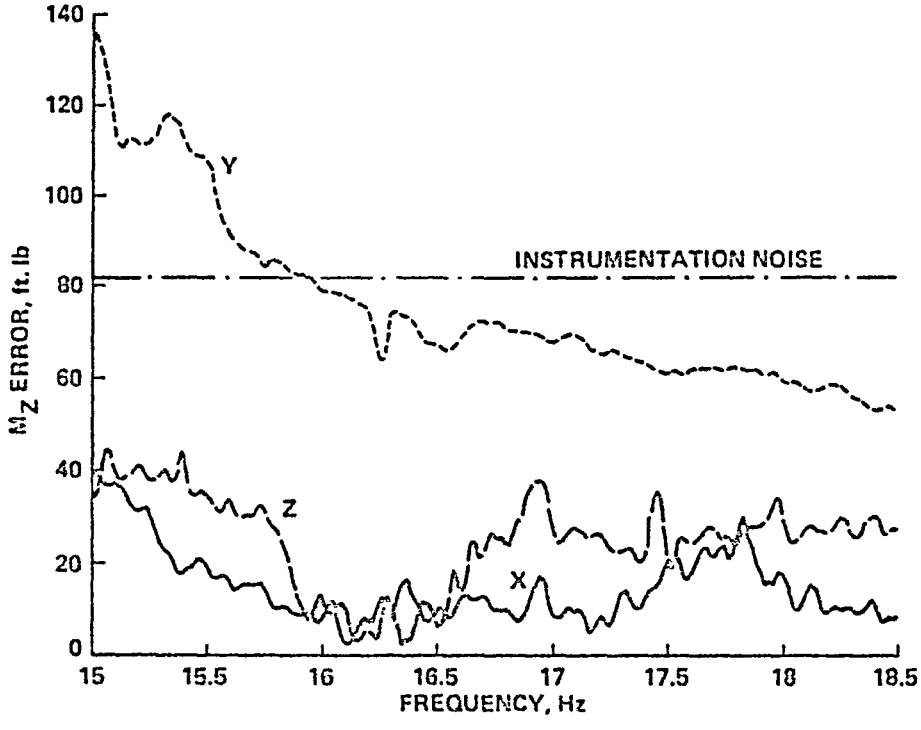

Figure 17 Comparison of magnitude of z-axis moment estimation error for applied x, y and z axis loads

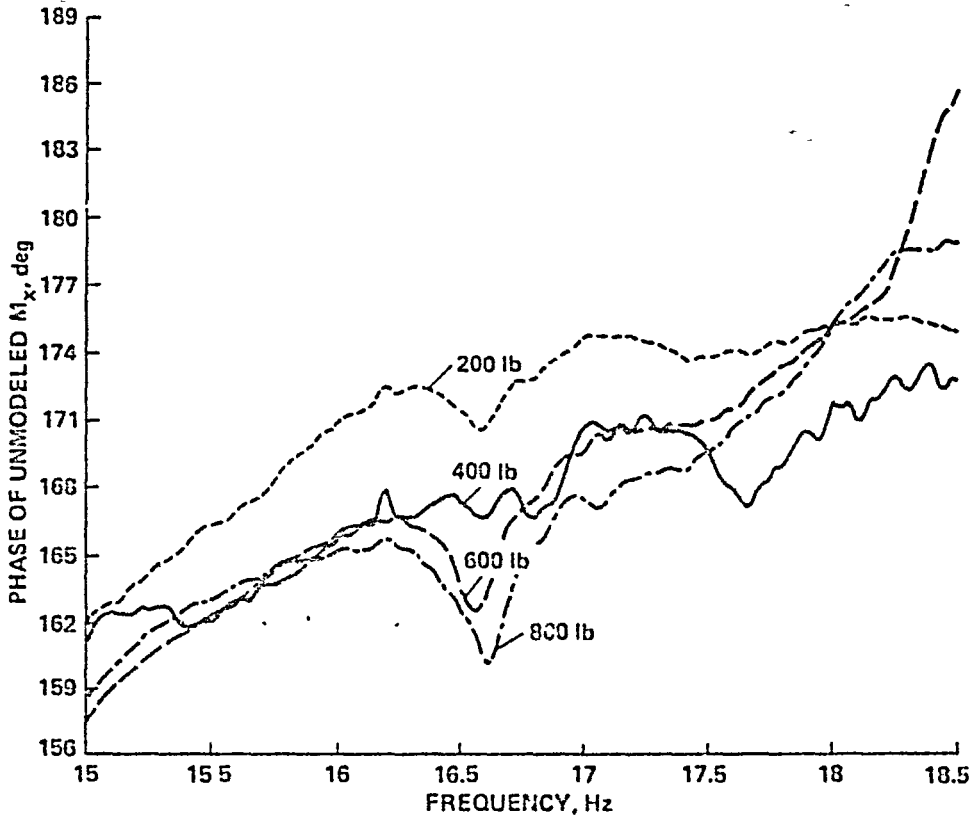

Figure 18 Phase lag unmodeled roll moment for applied lateral loads

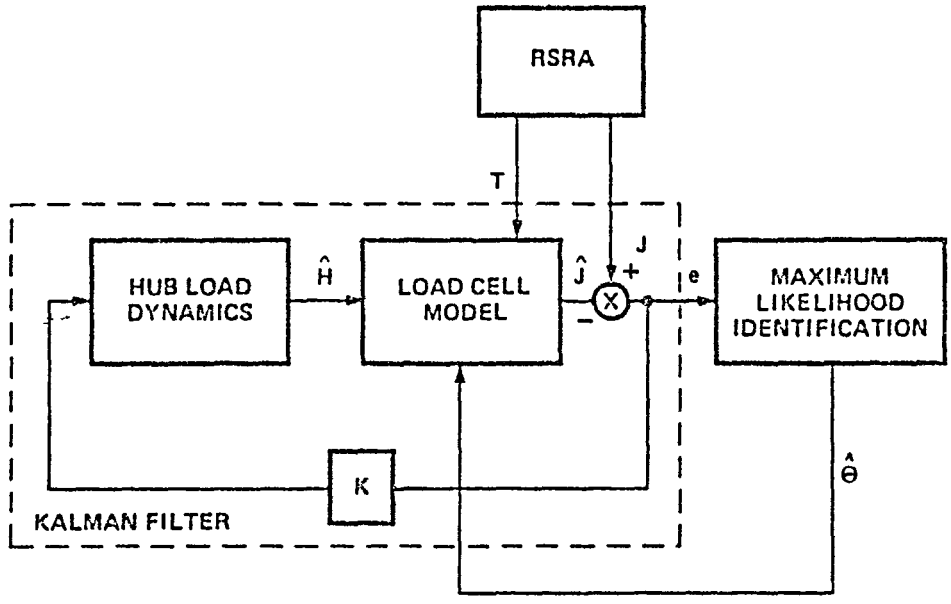

Figure 19 Schematic diagram of on-line calibration

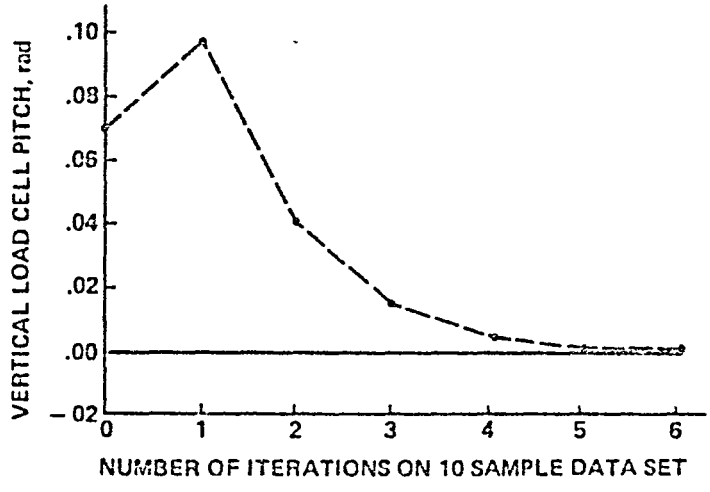

Figure 20 Identification of vertical load cell angle

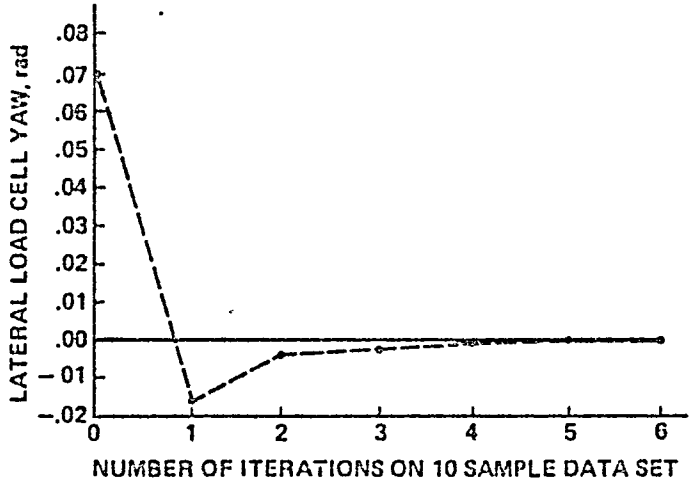

Figure 21 Identification of lateral load cell angle

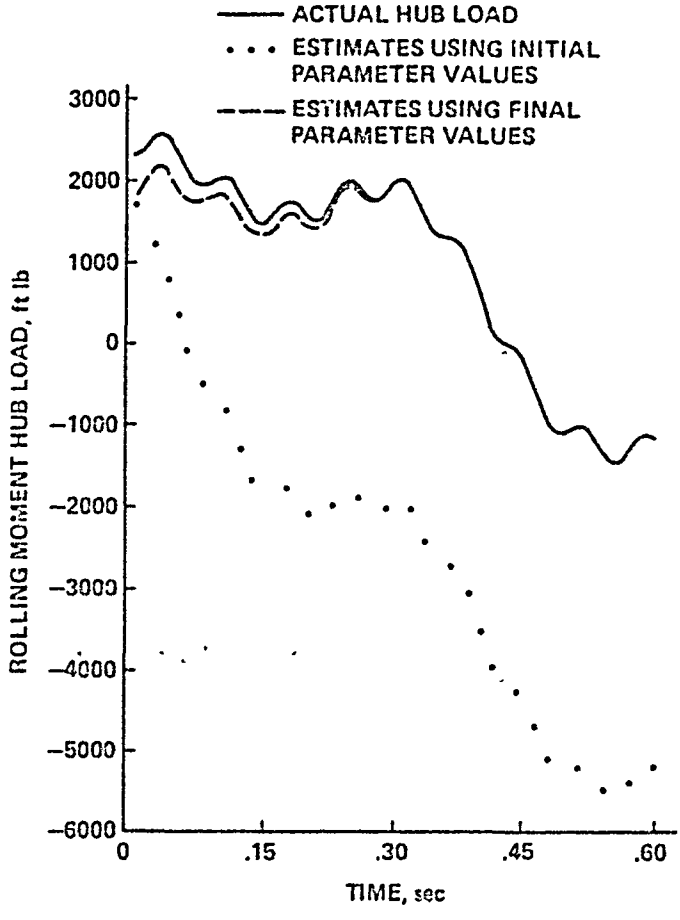

Figure 22 . Comparison of actual and estimated y-axis hub loads

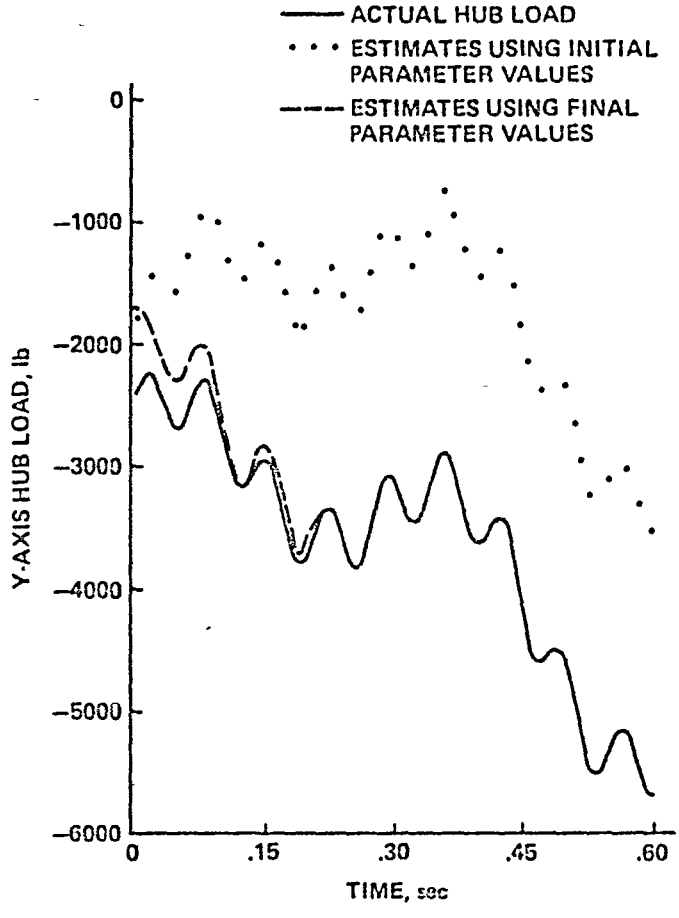

Figure 23 Comparison of actual and estimated rolling moment hub loads.

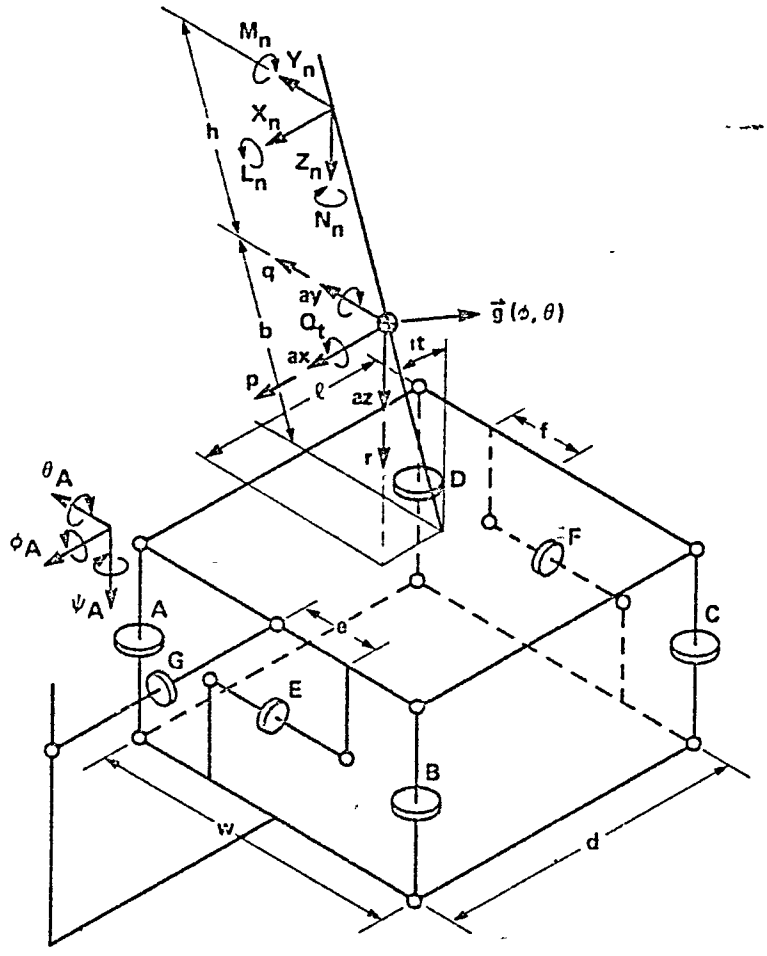

Figure A 1 Undeformed load cell geometery with generalized reaction force

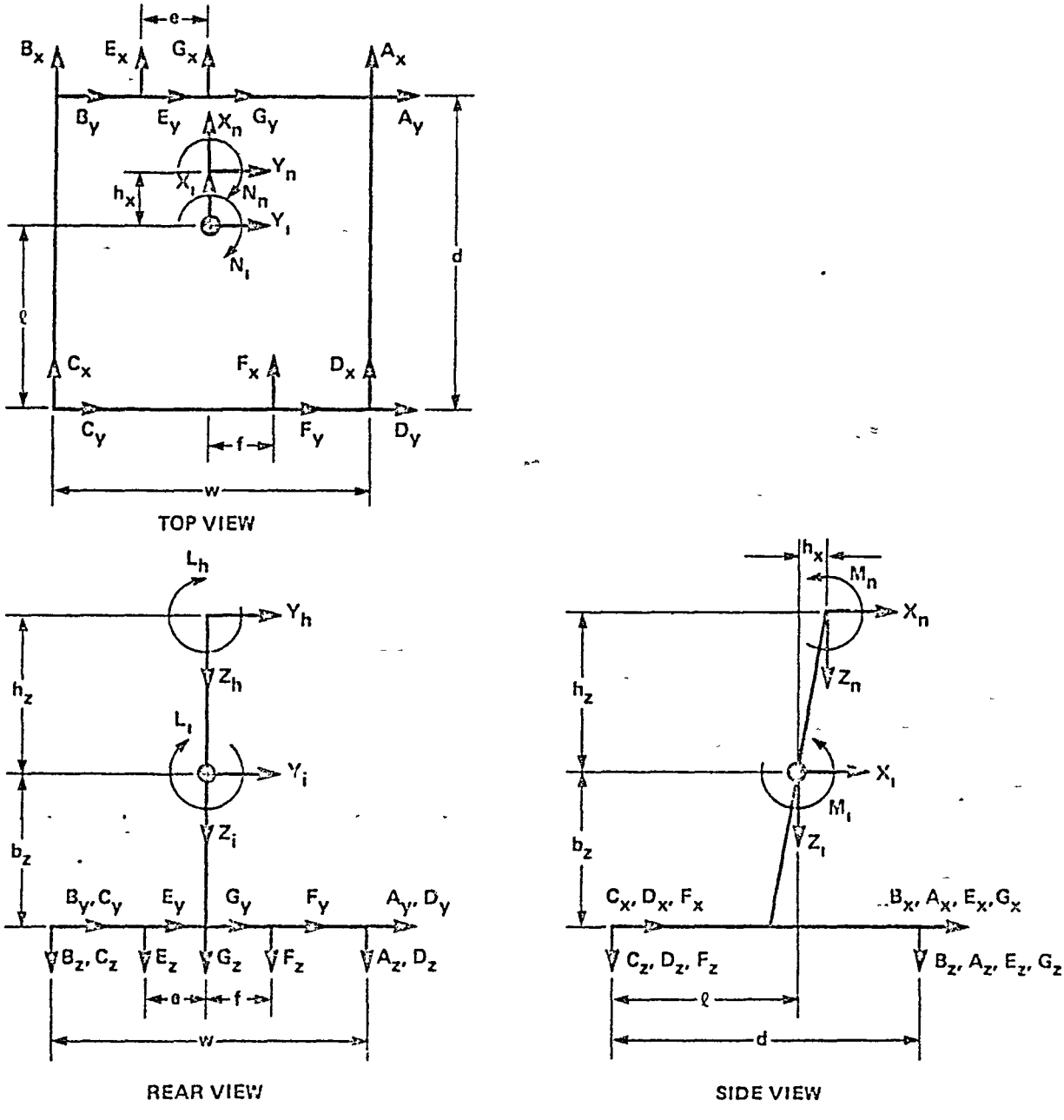

Figure A 2 Load cell geometry with generalised reaction force components

End of Document